The ER protein translocation channel subunit Sbh1 controls virulence of *Cryptococcus neoformans*

Felipe H. Santiago-Tirado[a,*], Thomas Hurtaux[a], Jennifer Geddes-McAlister[b], Duy Nguyen[c,**], Volkhard Helms[c], Tamara L. Doering[a,#], and Karin Römisch[d,#]

[a] Department of Molecular Microbiology, Washington University Medical School, St. Louis, Missouri, USA; fsantiago@nd.edu; thomas.hurtaux@wustl.edu; doering@wustl.edu

[b] Department of Molecular and Cellular Biology, University of Guelph, Ontario, Canada; jgeddesm@uoguelph.ca

[c] Center for Bioinformatics, Faculty of Natural Sciences and Technology, Saarland University, Saarbruecken, Germany; volkhard.helms@bioinformatik.uni-saarland.de

[d] Department of Biology, Faculty of Natural Sciences and Technology, Saarland University, Saarbruecken, Germany; k.roemisch@mx.uni-saarland.de

[*] Current address: Department of Biological Sciences, University of Notre Dame, Notre Dame, IN, USA

[**] Current address: DKFZ Heidelberg, Germany; duy.nguyen@dkfz-heidelberg.de

[#] Corresponding authors: k.roemisch@mx.uni-saarland.de
phone: +49-681-302 2704; ORCID ID 0000-0003-0415-6558

doering@wustl.edu
phone +1-314-747-5597; ORCID ID 0000-0002-5179-7393

Running title: Sbh1-dependence of *Cryptococcus neoformans* virulence

Abstract: 222 words (250 max)

Importance: 150 words (150 max)

Other text: 4790 words (excluding references, table notes, figure legends)

Abstract

The fungal pathogen *Cryptococcus neoformans* is distinguished by a cell wall-anchored polysaccharide capsule that is critical for virulence. Biogenesis of both cell wall and capsule relies on the secretory pathway. Protein secretion begins with polypeptide translocation across the endoplasmic reticulum (ER) membrane through a highly conserved channel formed by three proteins: Sec61, Sbh1, and Sss1. Sbh1, the most divergent, contains multiple phosphorylation sites, which may allow it to regulate entry into the secretory pathway in a species- and protein-specific manner. Absence of *SBH1* causes a cell-wall defect in both *Saccharomyces cerevisiae* and *C. neoformans*, although other phenotypes differ. Notably, proteomic analysis showed that when cryptococci are grown in conditions that mimic aspects of the mammalian host environment (tissue culture medium, 37 °C, 5% CO_2), a set of secretory and transmembrane proteins is upregulated in wild-type, but not in Δ*sbh1* mutant cells. The Sbh1-dependent proteins show specific features of their ER targeting sequences that likely cause them to transit less efficiently into the secretory pathway. Many also act in cell-wall biogenesis, while several are known virulence factors; consistent with these observations, the *C. neoformans* Δ*sbh1* mutant is avirulent in a mouse infection model. We conclude that, in the context of conditions encountered during infection, Sbh1 controls the entry of virulence factors into the secretory pathway of *C. neoformans*, and thereby regulates fungal pathogenicity.

Importance

Cryptococcus neoformans is a yeast that causes almost 200,000 deaths worldwide each year, mainly of immunocompromised individuals. The surface structures of this pathogen, a protective cell wall surrounded by a polysaccharide capsule, are made and maintained by proteins that are synthesized inside the cell and travel outwards through the secretory pathway. A protein called Sbh1 is part of the machinery that determines which polypeptides enter this export pathway. We found that when Sbh1 is absent, both *C. neoformans* and the model yeast *S. cerevisiae* show cell wall defects. Lack

of Sbh1 also changes the pattern of secretion of both transmembrane and soluble proteins, in a manner that depends on characteristics of their sequences. Notably, multiple proteins that are normally upregulated in conditions similar to those encountered during infection, including several needed for cryptococcal virulence, are no longer increased. Sbh1 thereby regulates the ability of this important pathogen to cause disease.

65 **INTRODUCTION**

66 *Cryptococcus neoformans* is a haploid budding yeast that is ubiquitous in the environment, so that
67 spores or dessicated cells are frequently inhaled (1, 2). In healthy individuals these infectious
68 particles are generally cleared or establish an asymptomatic latent infection (3). If, however, the
69 host is or becomes severely immunocompromised, the pathogen may grow and disseminate, both
70 within and outside of host cells (4). Dissemination to the central nervous system results in a
71 devastating meningitis, which causes almost 200,000 deaths each year worldwide (5).

72

73 Like other fungi, *C. neoformans* is protected by a multilayer cell wall, which is composed of a
74 meshwork of chitin, chitosan, alpha and beta glucans, and mannoproteins (6). This flexible and
75 dynamic structure responds to and protects the cell from environmental stresses, while
76 accommodating morphogenesis. An additional role of the cryptococcal wall is to anchor an
77 elaborate polysaccharide capsule that surrounds the cell (7, 8). This structure, which is unique
78 among fungal pathogens, is required for cryptococcal virulence (1). Capsule polysaccharides are
79 also shed from the cell into the surrounding environment, where they act to perturb the host
80 immune response (9, 10).

81

82 The biogenesis of both cell wall and capsule in *C. neoformans* relies on the secretory pathway,
83 which begins with protein translocation across the ER membrane through the highly conserved
84 Sec61 channel (11). An N-terminal hydrophobic signal peptide or a transmembrane domain targets
85 proteins to this channel, which is formed by three proteins: Sec61, Sbh1, and Sss1 in yeast (Fig. 1A)
86 and Sec61α, Sec61ß, and Sec61γ in mammals (11, 12). *SEC61* and *SSS1* are essential in *S.*
87 *cerevisiae* (13, 14). The 10 transmembrane helices of Sec61 form a protein-conducting channel in
88 the ER membrane, stabilized by Sss1 which clamps around the Sec61 helix-bundle (Fig. 1A) (12,
89 15, 16). *SBH1* and its paralog *SBH2* are not essential, but deletion of both genes leads to
90 temperature-sensitivity at 37°C in *S. cerevisiae* (17, 18). Sbh1/Sec61ß is a tail-anchored protein

91 associated peripherally with the Sec61 channel (19) (Fig. 1A). Its conserved transmembrane domain
92 is sufficient to rescue the double mutant growth defect at 37°C, while the role of its divergent
93 cytosolic domain containing multiple phosphorylation sites is poorly understood (18, 20, 21). As is
94 common for proteins with intrinsically unstructured domains, Sbh1/Sec61ß has multiple interactors:
95 it binds to ribosomes and mediates association of the Sec61 channel with signal peptidase and signal
96 recognition particle receptor (22, 23, 24, 25). In mammalian cells, the Sbh1 homolog Sec61ß also
97 interacts with the Stimulator of Interferon Genes (STING); this interaction is required for STING's
98 ability to stimulate interferon expression, thus linking the Sec61 channel to the innate immune
99 response (26). Sec61 with Sss1 can translocate proteins into the ER on its own, but the cytosolic
100 domain of Sec61ß contacts secretory proteins prior to insertion in the cytosolic vestibule of the
101 Sec61 channel and the presence of Sec61ß stimulates import (23, 27, 28). Recently, null mutations
102 in human SEC61B were identified as a cause for polycystic liver disease (29). The mutations led to
103 a complete biogenesis defect specific for polycystin-1, a large complex transmembrane protein with
104 a weak secretory signal sequence (29). Collectively, these data have led to the view that
105 Sbh1/Sec61ß mediates interaction of the Sec61 channel with other proteins in the ER membrane and
106 that its cytosolic domain aids insertion of specific signal peptides or transmembrane domains into
107 the Sec61 channel.
108
109 Phosphorylation is a frequent biological mechanism for regulation of protein activity or protein-
110 protein interactions and a systematic analysis identified 63 kinases that play a role in the
111 pathogenicity of *C. neoformans* (30, 31). One of these, Protein Kinase A (PKA), regulates the
112 secretion of a subset of virulence factors (32). Regulation of protein secretion may be important
113 during physiological transitions such as cell differentiation or development. Indeed Sec61ß - the
114 only subunit of the Sec61 channel that has been found to be phosphorylated so far - is important for
115 polarization of epithelial cells, and for development of *Drosophila melanogaster* embryos (33, 34,
116 35, 36). Both mammalian Sec61ß and yeast Sbh1 are phosphorylated at multiple sites in various

117 combinations (33, 21; phosphosite databases). The phosphorylation sites all lie in the intrinsically
118 unstructured cytosolic domain, and are not positionally conserved, with one exception: the proline-
119 flanked site at T5 in *S. cerevisiae* is present in mammals and some birds, although not in lower
120 vertebrates, invertebrates, or other non-pathogenic yeast species. This suggests that this
121 phosphorylation site evolved at least twice by convergent evolution and thus likely has an important
122 function (Fig. 1A, asterisk Fig. 1B) (21).
123
124 The 63 kinases required for virulence of *C. neoformans* include many proline-directed kinases (31,
125 37). When we aligned the N-termini of Sbh1 proteins from non-pathogenic and pathogenic yeast,
126 we noticed that - with the exception of *Candida albicans* - all pathogen Sbh1 proteins contain one
127 or more potential proline-flanked phosphorylation site(s) in the N-terminal cytosolic domain,
128 whereas Sbh1 proteins from non-pathogenic yeast species (*Schizosaccharomyces pombe,*
129 *Kluyveromyces lactis, Yarrowia lipolytica, Pichia pastoris, Hansenula polymorpha*) and the *S.*
130 *cerevisiae* homolog Sbh2 did not (Fig. 1B, pink; see Supplementary Figure 1 for full alignments).
131 This led us to hypothesize that these phosphorylation sites in Sbh1 might be connected to virulence
132 of the respective pathogenic species. In *C. neoformans* Sbh1 the proline-flanked phosphorylation
133 sites are preceded by a potential PKA phosphorylation site (Fig. 1B, blue) and secretion of a subset
134 of virulence factors in *C. neoformans* depends on PKA (32). We therefore decided to investigate the
135 role of Sbh1 and its N-terminal phosphorylation sites in virulence of *C. neoformans*.
136
137 We found that, unlike in *S. cerevisiae,* mutations of the N-terminal Sbh1 phosphorylation sites
138 (individually or in combination) do not affect *C. neoformans* growth in rich medium (YPD), and
139 that even complete deletion of *SBH1* only inhibits growth when combined with high temperature
140 and or cell wall stressors. We also observed that in infection-like conditions the deletion mutant
141 fails to properly regulate protein secretion; we have identified the Sbh1-dependent substrates and
142 identified common characteristics of their ER-targeting sequences. Notably, the affected proteins

143 include multiple virulence factors and the mutant is consequently avirulent in a mouse model of
144 infection. Together, our results show that Sbh1 is critical for secretion of a subset of virulence
145 factors and other proteins during *C. neoformans* infection, and is therefore essential for its
146 pathogenicity.
147
148 **RESULTS**
149 Sbh1 is required for cell wall integrity in *S. cerevisiae* and *C. neoformans*
150 We first looked to the best characterized system, *S. cerevisiae*. In this organism, both genes that
151 encode the Sec61 channel beta subunit (*SBH1* and *SBH2*) are required for growth on YPD at 37°C
152 (Fig. 1C) (17, 18, 21). *S. cerevisiae* lacking *SBH1* and *SBH2* are also resistant to calcofluor white
153 (Fig. 1D), which suggests either reduced chitin in the cell wall or altered cell wall architecture.
154 Further, we observed increased extractability of proteins from the cell wall by alkaline buffer
155 containing dithiotreitol, which also suggests structural defects in the wall (Fig. 1E). While mutation
156 of the conserved Sbh1 phosphorylation site T5 to A on its own has no effect on *S. cerevisiae* growth
157 or cell wall integrity (21), mutation of both proline-flanked phophorylation sites to A phenocopied
158 the absence of Sbh1 in *S. cerevisiae*. Mutation of both residues to phosphomimetic E had no effect
159 (Fig. 1D, E).
160
161 The phenotypes we observed in *C. neoformans* cells lacking their sole *SBH1* gene were quite
162 distinct from those of *S. cerevisiae*. Specifically, they showed only subtle temperature sensitivity at
163 37°C on YPD (Fig. 2A, left panel) and no sensitivity to osmotic or cell wall stressors at 30°C (Fig.
164 2A). At 37°C, however, the mutant cells were hypersensitive to SDS and barely grew on calcofluor
165 white (Fig. 2A, lower panels; Fig. 2B, top two rows); they were also more sensitive than wild-type
166 cells to cell wall digestion by lysing enzymes (Fig. 2C) and showed increased sensitivity to
167 oxidative stress (1 mM H_2O_2; Fig. 2D, top two rows), which is encountered in the setting of
168 infection. Overall, we conclude that Sbh1 is required for cell wall integrity in both the ascomycete

169 *S. cerevisiae* and the basidiomycete *C. neoformans*, although specific manifestations of this
170 requirement differ (see Discussion).
171
172 Sbh1 N-terminal phosphorylation sites do not affect cell wall integrity in *C. neoformans*
173 As discussed above, we hypothesized that the N-terminal phosphorylation sites in cryptococcal
174 Sbh1 were important for protein function. To test this, we first engineered a plasmid to express
175 wildtype *SBH1* modified with a C-terminal HA tag. The tagged protein effectively complemented
176 the sensitivity of *sbh1*Δ mutants to cell wall stressors (CFW and SDS, Figure 2B). We then
177 modified this expression plasmid to encode Sbh1 that was altered to eliminate either the putative
178 PKA site (Ser8 to Ala), two proline-flanked phosphorylation sites (Ser9 to Ala and Thr12 to Val),
179 or all three sites. All of these polypeptides were expressed at similar levels, except for the version
180 with a sole PKA site mutation, which was slightly less abundant (Supplementary Figure 2). We
181 found that each of the mutated proteins fully complemented growth of *sbh1*Δ cells in the presence
182 of CFW and also restored growth at 37 °C in the presence of SDS (Fig. 2B). Interestingly, cells
183 expressing mutant versions of Sbh1 grew slightly better on YPD and were more resistant to SDS
184 than those expressing the WT protein (Fig. 2B). Each mutant protein also completely
185 complemented the defective growth of the *sbh1*Δ mutant in the presence of oxidative stress (Fig.
186 2D). Together, these results suggest that, surprisingly, these phosphorylation sites are not required
187 for Sbh1 function, as assessed by its role in cell wall integrity.
188
189 Sbh1-dependent secretory and transmembrane proteins are induced in conditions that mimic the
190 host environment
191 Sbh1 contacts signal peptides in the cytosolic vestibule of the Sec61 channel, so it can both guide
192 secretory proteins into the channel and control their access to the secretory pathway. To address
193 whether biogenesis of specific secretory or transmembrane proteins was compromised in the
194 absence of *C. neoformans* Sbh1, we analyzed the proteomes of wild-type and *sbh1*Δ cells grown in

195 either rich medium (YPD) at 30°C or in DMEM at 37°C and 5% CO_2. The latter, termed 37D5
196 below, was chosen to mimic key features of the complex host environment. We detected no
197 significant differences between wildtype KN99 and *sbh1*Δ strains in YPD at 30°C (Fig. 3),
198 suggesting no critical role for Sbh1 in those conditions. In 37D5, however, we discovered a set of
199 proteins that was specifically induced in wild-type cells, but not in the *sbh1*Δ mutant (Fig. 3,
200 Supplementary Table 1). This set included 32 proteins without secretory pathway targeting
201 sequences, 21 transmembrane (TM) proteins and 68 proteins with signal peptides (SP) or uncleaved
202 signal anchors (SA) (Supplementary Table 1). When we analyzed their ER-targeting sequences we
203 found that the transmembrane domains were slightly more hydrophobic than average for
204 transmembrane proteins in *C. neoformans*; many also had a strong positively charged patch in close
205 proximity to one side of the TM domain (Fig. 4A; Supplementary Table 2). Some of the
206 transmembrane domains of the Sbh1-dependently induced proteins also contained a high number of
207 prolines and/or glycines in addition to the polybasic stretch adjacent to the transmembrane domain
208 (Supplementary Table 2). The Sbh1-dependent signal peptides were more heterogeneous, but most
209 displayed reduced C-region polarity (Fig. 4B; Supplementary Table 2). In addition, they were
210 suboptimal in various ways which therefore defied bioinformatic analysis: some had limited
211 hydrophobicity, some contained high numbers of proline and glycine which interfere with alpha-
212 helix formation, and many had a charge bias problem (either no charge on either side of the
213 hydrophobic core, or a positive charge C-terminal instead of N-terminal of the hydrophobic core, or
214 multiple positive charges at the N-terminus of the mature part of the protein) (Supplementary Table
215 2). Because signal peptides insert as alpha-helices into the hydrophobic lateral gate of the Sec61
216 channel with the positively charged N-terminus towards the cytosol, any of these features will
217 reduce translocation efficiency into the ER. We suggest that Sbh1 is required for the biogenesis of
218 specific secretory and transmembrane proteins under host-like conditions. Our model is that because
219 the targeting sequences of these proteins are suboptimal for Sec61 channel insertion, they rely on
220 the enhanced insertion efficiency provided by the presence of Sbh1 (Fig. 4C) (23).

221

222 Sbh1 is essential for virulence of *C. neoformans*

223 The proteome analysis presented above shows that Sbh1 regulates the secretion of proteins that are
224 induced by host-like conditions. This process is likely important for pathogenesis, as supported by
225 our observation that *sbh1*Δ cells have a reduced ability to survive within host macrophages (Figure
226 5, panels A and B). To directly test the role of Sbh1 in virulence, we used a well-established mouse
227 model for cryptococcal infection. At 14 days after intranasal infection we observed a striking
228 reduction in both lung and brain fungal burden in *sbh1*Δ-infected animals compared to wild type
229 (Figure 5, panels C and D). Consistent with this finding, mice infected with wild-type cryptococci
230 succumbed to infection within 18 days, while mutant-infected animals remained healthy and grew
231 normally for at least 10 weeks (Figure 5, panels E and F). We conclude that *SBH1* is essential for *C.*
232 *neoformans* virulence.

233 **DISCUSSION**

234 In this work we sought to identify factors regulating secretion of virulence-relevant proteins in the
235 human pathogen *C. neoformans*. We specifically investigated the role of the non-essential ER
236 protein translocation channel subunit Sbh1. Since the Sbh1 cytosolic domain contacts secretory
237 signal sequences in the cytosolic vestibule of the channel prior to insertion into the channel it can
238 potentially aid or restrict protein import into the secretory pathway of specific proteins under
239 specific growth conditions. This may be regulated by phosphorylation as Sbh1 in all species
240 contains multiple phosphorylation sites which are only partially positionally conserved (Fig. 1A, B).
241

242 In *S. cerevisiae*, absence of *SBH1* and its paralog *SBH2* causes temperature sensitivity, although the
243 ER translocation defects at the restrictive temperature are modest for most substrates investigated
244 (Fig. 1C; 38, 18). We hypothesized that this phenotype could relate to defects in the cell wall for
245 several reasons: other translocation mutants exhibit cell wall defects (39); wall synthesis relies on
246 secretory proteins; and alterations in this process often yield a temperature-sensitive phenotype (40).
247 We investigated the effect of *sbh1* mutants on cell wall integrity by assessing growth on calcofluor
248 white (CFW; Fig 1D) and extractability of cell wall proteins by high pH/dithiotreitol treatment (Fig.
249 1E). CFW binds to chitin in the yeast cell wall and is toxic (41). *KRE6* encodes a glucosyl hydrolase
250 required for beta-1,6-glucan synthesis; the deletion mutant is hypersensitive to CFW and is shown
251 as a control. Cells lacking Sbh1 were slightly resistant to CFW (Fig. 1D), indicating a reduced
252 amount of chitin in the cell wall, and displayed increased extraction of cell wall proteins (Fig. 1E).
253 *S. cerevisiae* cell wall integrity also specifically required the two proline-flanked N-terminal
254 phosphorylation sites at S3 and T5; mutation of these residues to non-phosphorylatable A
255 phenocopied the cell wall defects of the deletion mutant (Fig. 1D, E). The *sbh1 S3E/T5E* mutant
256 behaved like wildtype (Fig. 1D, E). Proline-flanked phosphorylation sites in Sbh1 of other yeast
257 species occur primarily in human pathogens (Fig. 1B), which suggested to us that phosphorylation
258 at these sites may play a regulatory role in virulence. The absence of *SBH1* in *C. neoformans*

259 resulted only in a very modest temperature sensitivity at 37°C (Fig. 1C vs. 2A), although at high
260 temperature *sbh1*Δ *C. neoformans* also displayed a cell wall defect (Fig. 2A-C). In contrast to *S.*
261 *cerevisiae*, however, mutation of the N-terminal proline-flanked phosphorylation sites of *C.*
262 *neoformans* Sbh1 individually or in combination did not phenocopy the cell wall defect (Fig. 2B).
263 As protein kinase A has been shown to be critical for *C. neoformans* virulence, and *C. neoformans*
264 Sbh1 also contains a PKA site (Fig. 1B, blue), we also mutated this site alone or in combination
265 with the proline-flanked sites, but again saw no effect on cell wall integrity (Fig. 2B) (32).
266 Surprisingly, the altered phosphorylation sites slightly enhanced cell growth, especially notable on
267 SDS (Fig. 2B). Taken together, our data suggest that Sbh1 is important for efficient secretion of one
268 or more enzymes or precursors for the cell wall in both *S. cerevisiae* and in *C. neoformans*, but that
269 the role of the N-terminal proline-flanked phosphorylation sites in this process differs in the two
270 organisms. Alternatively, the differential effect of the phosphorylation site mutations may reflect
271 their distinct cell wall compositions: whereas the *S. cerevisiae* cell wall is formed by ß-1,3-glucan,
272 ß-1,6-glucan, chitin, and mannoproteins, in the *C. neoformans* cell wall most chitin is deacylated to
273 chitosan, and α-1,3-glucan is a major cell wall component (42, 10).
274
275 We next asked which proteins were affected by absence of *SBH1* in *C. neoformans*. Using a
276 proteomic approach we identified a set of secretory and transmembrane proteins that were induced
277 under 37D5 conditions in the wild-type strain, but not in the *sbh1*Δ mutant (Fig. 3; Supplementary
278 Tables S1 and S2). Many of the membrane proteins in this set were characterized by a strong
279 polybasic patch adjacent to the first transmembrane domain (e.g. CNAG_1854, CNAG_5502,
280 CNAG_6416), while the signal peptides of the secretory proteins were more heterogeneous, and had
281 less polar C-regions than average (Supplementary Table S2; Fig. 4A, B). This is reminiscent of the
282 ER targeting signals identified by Ziska and colleagues in mammalian cells whose ER import was
283 dependent on the Sec61 channel-interacting protein Sec63 and the ER-lumenal Hsp70 chaperone
284 BiP (43). In *S. cerevisiae* the Sec63 complex composed of Sec63, Sec62, Sec71, and Sec72

285 promotes posttranslational protein import into the ER through the Sec61 channel by stabilizing the
286 lateral gate in a partially open conformation (44, 12). It also plays a role in membrane protein
287 topogenesis in both yeast and mammalian cells (45, 46). Sec63 is a polytopic membrane protein
288 with an ER-lumenal J-domain that activates ATP-hydrolysis of the ER-lumenal chaperone BiP
289 (Kar2 in yeast) (47). Kar2 contributes to protein import into the ER either by directly binding to the
290 incoming protein or by promoting its folding (48, 49). As proteins dependent on Sbh1 in *C.*
291 *neoformans* and proteins dependent on Sec63/BiP in mammalian cells have similar characteristics,
292 our data suggest that Sbh1 and the Sec63 complex have overlapping functions in promoting ER
293 import of specific proteins.
294
295 Signal peptides generally insert into the Sec61 channel with their N-terminus towards the cytosol
296 and their N-terminal positive charge (Fig 4B, '+') contributes to this orientation (50). Many of the
297 Sbh1-dependent signal peptides we identified in *C. neoformans* have no charge bias towards the N-
298 terminus; in some, the charge bias is even reversed (Supp. Table S2). Sbh1 may help orient such
299 signal peptides in the cytosolic vestibule of the Sec61 channel with the help of its cytosolic domain.
300 The polar C-region of signal peptides contains the signal peptidase cleavage site (50). Most of the
301 Sbh1-dependent signal peptides we identified have a very short C-region (Supp. Table S2) which
302 may limit signal peptidase access unless the signal peptide is positioned accurately by Sbh1. In
303 order to efficiently insert into the Sec61 channel the signal peptides of secretory proteins require an
304 alpha-helical hydrophobic region (Fig 4B, H region, blue) (50). Many of the Sbh1-dependent signal
305 peptides of *C. neoformans* contain multiple helix-breaking P or G residues within their hydrophobic
306 helical core regions, and some have very short or very long hydrophobic H-regions (Supp. Table 2).
307 These features would make it difficult for signal peptides to stably insert into the Sec61 channel
308 lateral gate. Overexpression of an N-terminally truncated Sbh1 lacking most of its cytosolic domain
309 complements the temperature-sensitivity and at least some of the translocation defect in Δ*sbh1*
310 Δ*sbh2 S. cerevisae* (18). Together with our data, this suggests that the Sbh1 transmembrane domain

311 stabilizes a conformation of the Sec61 lateral gate that favours insertion of the helical hydrophobic
312 core of signal peptides, even if they are suboptimal.
313
314 That Sbh1-dependent secretion is critical for virulence is illustrated by both the reduced intracellular
315 fitness of *sbh1*Δ *C. neoformans* in macrophages and the effects in mice. In contrast to infection with
316 KN99 wildtype *C. neoformans*, which resulted in a high burden in the lungs and death of all mice
317 by day 18 post infection, all mice infected with *sbh1*Δ *C. neoformans* survived for 70 days and even
318 gained weight (Figure 5), showing that the mutant strain was avirulent.
319
320 We hypothesize that the striking defect in virulence of the *sbh1* mutant reflects reduced secretion of
321 multiple groups of proteins. For a few examples, these could include proteins required for fungal
322 growth in the host environment (e.g. metabolic genes or proteins involved in cell wall synthesis),
323 needed for virulence factor production, or directly involved in host damage. These categories may
324 also interact; for example, mutations that alter cell wall glycan synthesis also result in aberrant
325 formation of the capsule (7, 8, 51, 52). To explore this idea, we reviewed the polypeptides whose
326 secretion is most impaired in the absence of Sbh1 (Supplementary Table 1), focusing on proteins
327 with signal or transmembrane sequences that had been previously implicated in cryptococcal
328 virulence. We identified eight such proteins, which had exhibited infectivity defects in a large-scale
329 screen (53) and/or been individually studied and shown to contribute to virulence (Table 1). One of
330 them, Cig1, has also been detected in the blood of mice infected with *C. neoformans*, leading to the
331 suggestion that it could serve as a biomarker of infection (32). Notably, all of the corresponding
332 genes are expressed in human CSF during cryptococcal meningitis, most at higher levels than in
333 rich medium (Table 1 and (54)). Two proteins in this group (Pbx1(55,56) and Skn1 (57)) act in cell
334 wall synthesis, so their reduced secretion could contribute to the wall defects and sensitivity to
335 host-induced stress that we observed in *sbh1* mutant cells. Another is required for capsule display
336 (Cap60 (58)), although its biochemical function has not been characterized, and two others are

337 proteases (CNAG_00150 and Mpr1 (59)). Many fungal proteases damage host tissues during
338 infection (60) and Mpr1 further acts in cryptococcal crossing of the blood-brain barrier (59), which
339 is required for cryptococcal dissemination to the brain and subsequent lethality. Supporting a role
340 in infection for this group of proteins, six of the corresponding genes are expressed more highly in
341 37D5 than in rich medium (one other is modestly decreased); this pattern is particularly striking for
342 *CIG1* and *MPR1*, whose expression levels increase over 100-fold (Table 1) (61). Notably, the
343 evidence that these proteins are important for cryptococcal virulence derives from studies of
344 individual gene deletion strains, which completely lack one of these target proteins. The situation in
345 the *sbh1* mutant is different, in that many proteins are secreted less efficiently, but none (besides
346 Sbh1) are absent. Nonetheless, the impaired secretion of multiple proteins with key roles in
347 virulence, together with others in the functional groups above, provides abundant reason for the
348 inability of *sbh1* to cause disease in a mammalian host.

349

350 We conclude that *C. neoformans* Sbh1 is important for biogenesis of virulence factors whose
351 specific ER-targeting sequences make these proteins dependent on Sbh1 for ER import (Fig. 4C).
352 Recently, Sec61beta has also been shown to be critical for infection by the important fungal crop
353 pathogen *Magnaporthe oryzae*, suggesting a more general role for Sbh1/Sec61beta in fungal
354 infection (62). Since the intrinsically unstructured N-terminal part of the Sbh1 cytosolic domain is
355 not conserved between yeast and mammals, our work may suggest a new specific target for
356 developing drugs against this important human pathogen.

357

358 **MATERIALS AND METHODS**

359 *S. cerevisiae* methods

360 *S. cerevisiae* strains are detailed in the Supplemental Methods and were grown on either yeast
361 peptone dextrose (YPD) or synthetic complete medium without leucine, with or without 10 µg/ml
362 calcofluor white (Sigma), at 30°C or 37°C, for 3 days. Cell wall proteins were extracted from cells

363 in early exponential phase in 100 mM Tris-HCl, pH 9.4, 10 mM DTT at 37 °C, and TCA-
364 precipitated for SDS-PAGE analysis as detailed in the Supplemental Methods.
365
366 *C. neoformans* strains, growth conditions, and plasmids
367 All strains were in the *C. neoformans* serotype A strain KN99α background, as detailed in the
368 Supplemental Methods, and were grown at 30°C on YPD with 100 µg/mL of nourseothricin or
369 100 µg/mL G418 as appropriate. After plasmids expressing the native *SBH1* gene or version with
370 5 HA epitopes at the C-terminus were shown to complement phenotypic defects of the *sbh1*
371 mutant, the tagged version was mutagenized to modify N-terminal motifs and electroporated into
372 KN99α and the *sbh1*Δ strains as described in (63) and detailed in the Supplemental Methods.
373 Because of the heterogeneity in copy number associated with plasmids in *C. neoformans*, at least
374 three independent colonies were picked and tested for each construct; all exhibited the same
375 behaviors.
376
377 Phenotypic assays and mass spectrometry
378 Serial dilution plate assays and sensitivity to hypotonic lysis after exposure to lysing enzyme were
379 assessed as detailed in the Supplementary Methods and (64). Total cellular proteome analysis was
380 performed as in (65, 66) and the Supplementary Methods. Results were compared to the reference
381 *C. neoformans* reference proteome and deposited in the PRIDE partner repository for the
382 ProteomeXchange Consortium with the data set identifier: PXD013894. A Student's *t*-
383 test was performed to identify proteins with a significant differential expression (*p-value* < 0.05)
384 (S_0 = 1) between samples employing a 5% permutation-based FDR filter.
385
386 Infection assays
387 Fungal survival after engulfment by THP-1 (ATCC #TIB-202) cells *in vitro* was assessed as in
388 (67), with minor modifications detailed in the Supplemental Methods. For *in vivo* studies, 4-6

389 week-old female C57BL/6 mice were intranasally inoculated with $5x10^4$ cryptococcal cells and
390 either followed by weight for survival studies or sacrificed at set times for organ burden
391 measurement, as detailed in the Supplemental Methods. All animal studies were reviewed and
392 approved by the Animal Studies Committee of Washington University School of Medicine and
393 conducted according to the National Institutes of Health guidelines for housing and care of
394 laboratory animals.
395

396 **ACKNOWLEDGMENTS**

397 We thank William Allen, Bristol University, for help with Fig. 1A; Christina Soromani, Andrea
398 Ludes, and Nicole Spitzlberger (all former students of the Römisch lab) for data shown in Fig. 1C,
399 D; Alyssa R. Brunsmann, Daphne Ko, and Liza Loza for qPCR studies; and Jussi Jäntti, VTT
400 Helsinki, for *S. cerevisiae* strains and plasmids.
401

402 KR was funded by core funding of the Saarland University. Work in the Doering lab was supported
403 by NIH grants AI140979 and AI135012 to TLD. FHS also received support from NIH T32 grant
404 AI007172 and a Postdoctoral Enrichment Program Award from the Burroughs Wellcome
405 Fund. JGM is supported by the Canadian Foundation for Innovation (JELF #38798) and the
406 Canadian Institutes for Health Research (Project Grant). VH was supported by Deutsche
407 Forschungsgemeinschaft grant He3875/15-1. The funders had no role in study design, data
408 collection and interpretation, or the decision to submit the work for publication.
409

410 **DATA AVAILABILITY**

411 Proteomics .Raw data files are available in the PRIDE (Proteomics Identification Database):
412 Project ID: PXD013894
413 **Username:** reviewer78525@ebi.ac.uk
414 **Password:** 8ZiMfbKG

415 **REFERENCES**

416 1. Kwon-Chung K, Fraser, JA, Doering TL, Wang Z, Janbon G, Idnurm A, and Bahn YS (2014).
417 *Cryptococcus neoformans* and *Cryptococcus gattii,* the etiologic agents of cryptococcosis.
418 *Cold Spring Harbor perspectives in medicine* 4:a019760.
419 2. Srikanta D, Santiago-Tirado FH, and Doering TL (2014). *Cryptococcus neoformans*: historical
420 curiosity to modern pathogen. *Yeast* 31:47-60.
421 3. Montoya MC, Magwene PM, and Perfect JR (2021). Associations between Cryptococcus
422 Genotypes, Phenotypes, and Clinical Parameters of Human Disease: A Review. *J Fungi*
423 *(Basel)* 7: 260.
424 4. Gaylord EA, Choy HL, and Doering TL (2020). Dangerous Liaisons: Interactions of
425 *Cryptococcus neoformans* with Host Phagocytes. *Pathogens* 9:891-905.
426 5. Rajasingham R, Smith RM, Park BJ, Jarvis JN, Govender NP, Chiller TM, Denning DW, Loyse
427 A, and Boulware DR (2017). Global burden of disease of HIV-associated cryptococcal
428 meningitis: an updated analysis. *Lancet Infectious Dis* 17:873-881.
429 6. Loza L, and Doering TL (2021). Glycans of the pathogenic yeast *Cryptococcus neoformans* and
430 related opportunities for therapeutic advances. in *Comprehensive Glycoscience* (Barchi, J.
431 ed.), 2nd Ed., Elsevier.
432 7. Reese AJ, and Doering TL (2003). Cell wall alpha-1,3-glucan is required to anchor the
433 *Cryptococcus neoformans* capsule. *Mol Microbiol* 50:1401-1409.
434 8. Reese AJ, Yoneda A, Breger JA, Beauvais A, Liu H, Griffith CL, Bose I, Kim MJ, Skau C, Yang
435 S, Sefko JA, Osumi M, Latge JP, Mylonakis E, and Doering TL (2007). Loss of cell wall
436 alpha(1-3) glucan affects *Cryptococcus neoformans* from ultrastructure to virulence. *Mol*
437 *Microbiol* 63:1385-1398.
438 9. Agustinho DP, Miller LC, Li LX, and Doering TL (2018). Peeling the onion: the outer layers of
439 *Cryptococcus neoformans*. *Mem Inst Oswaldo Cruz* 113:e180040.

440 10. Wang ZA, Li LX, Doering TL (2018). Unravelling synthesis of the cryptococcal cell wall and
441 capsule. Glycobiology 28:719-730.
442 11. Voorhees R and Hegde RS (2016). Toward a structural understanding of co-translational
443 protein translocation. *Curr Opin Cell Biol* 41:91-99.
444 12. Wu X, *et al.* (2019) Structure of the post-translational protein translocation machinery of the
445 ER membrane. *Nature* 566:136-139.
446 13. Stirling CJ, Rothblatt J, Hosobuchi M, Deshaies R, Schekman R (1992). Protein translocation
447 mutants defective in the insertion of integral membrane proteins into the endoplasmic
448 reticulum. *Mol Biol Cell* 3:129–42.
449 14. Esnault Y, Blondel M, Deshaies R, Schekman R, Képès F (1993). The yeast SSS1 gene is
450 essential for secretory protein translocation and encodes a conserved protein of the
451 endoplasmic reticulum. *EMBO J* 12:4083–93.
452 15. Esnault, Y, Feldheim, D, Blondel, MO, Schekman, R, and Képès, F (1994). *SSS1* encodes a
453 stabilizing component of the Sec61 subcomplex of the yeast protein translocation apparatus. *J*
454 *Biol Chem* 269:27478–24785.
455 16. Falcone D, Henderson MP, Nieuwland H, Coughlan CM, Brodsky JL, Andrews DW (2011).
456 Stability and function of the Sec61 translocation complex depends on the Sss1p tail-anchor
457 sequence. *Biochem J* 436:291-303.
458 17. Toikkanen J, Gatti E, Takei K, Saloheimo M, Olkkonen VM, Söderlund H, de Camilli P,
459 Keränen S (1996). Yeast protein translocation complex: Isolation of two genes SEB1 and
460 SEB2 encoding proteins homologous to the Sec61ß subunit**.** *Yeast* 12:425-438.
461 18. Feng D, Zhao X, Soromani C, Toikkanen J, Römisch K, Vembar SS, et al (2007). The
462 transmembrane domain is sufficient for Sbh1p function, its association with the Sec61
463 complex, and interaction with Rtn1p. *J Biol Chem* 282:30618-28.
464 19. Leznicki P, Warwicker J, High S (2011). A biochemical analysis of the constraints of tail-
465 anchored protein biogenesis. *Biochem J* 436:719-727.

466 20. Leroux A, Rokeach LA (2008). Interspecies complementation of the translocon beta subunit
467 requires only its transmembrane domain. PLoS One 3(12):e3880.
468 21. Soromani C, Zeng N, Hollemeyer K, Heinzle E, Klein M-C, Tretter T, et al (2012). N-
469 acetylation and phosphorylation of Sec complex subunits in the ER membrane. *BMC Cell Biol*
470 13:34.
471 22. Levy R, Wiedmann M, Kreibich G (2001). *In Vitro* binding of Ribosomes to the ß subunit of
472 the Sec61p protein translocations complex. *J Biol Chem* 276:2340-2346.
473 23. Kalies K-U, Rapoport TA, Hartmann E (1998). The β subunit of the Sec61 complex facilitates
474 cotranslational protein transport and interacts with signal peptidase during translocation. *J Cell*
475 *Biol* 141:887–94.
476 24. Antonin W, Meyer HA, Hartmann E (2000). Interactions between Spc2 and other components
477 of the endoplasmic reticulum translocation sites of the yeast *Saccharomyces cerevisiae*. *J Biol*
478 *Chem* 275:34068-72.
479 25. Jiang Y, Cheng Z, Mandon EC, Gilmore R (2008). An interaction between the SRP receptor
480 and the translocon is critical during cotranslational protein translocation. *J Cell Biol* 180:1149-
481 1161.
482 26. Ishikawa H, Barber GN (2005). STING is an endoplasmic reticulum adaptor that facilitates
483 innate immune signalling. *Nature* 455:674-679.
484 27. Laird V, High S (1997). Discrete cross-linking products identified during membrane protein
485 biosynthesis. *J Biol Chem* 272:1983-1989.
486 28. Besemer J, Harant H, Wang S, Oberhauser B, Marquardt K, Foster SA, Schreiner EP, de Vries
487 JE, Dascher-Nadel C, Lindley IJD (2005). Selective inhibition of cotranslational translocation
488 of vascular cell adhesion molecule 1. *Nature* 436:290-93.
489 29. Besse W, Dong K, Choi J, Punia S, Fedeles SV, Choi M, Gallagher AR, Huang EB, Gulati A,
490 Knight J, ManeS, Tahvanainen E, Tahvanainen P, Sanna-Cherchi S, Lifton RP, Watnick T, Pei

491 YP, Torres VE, Somlo S (2017). Isolated polycystic liver disease genes define effectors of
492 polycystin-1 function. *J Clin Invest* 127:1772-85.
493 30. Ubersax JA, Ferrell JE jr (2007). Mechanisms of specifity in protein phosphorylation. *Nature*
494 8:530-542.
495 31. Lee KT, So YS, Yang DH, Jung KW, Chio J, et al. (2016). Systematic functional analysis of
496 kinases in the fungal pathogen *Cryptococcus neoformans*. *Nature Communications* 7:12766.
497 32. Geddes JMH, Croll D, Caza M, Stoynov N, Foster LJ, Kronstad JW (2015). Secretome
498 profiling of *Cryptococcus neoformans* reveals regulation of a subset of virulence-associated
499 proteins and potential biomarkers by protein kinase A. *BMC Microbiology* 15:206.
500 33. Gruss OJ, Feick P, Frank R, Dobberstein B (1999). Phosphorylation of components of the ER
501 translocation site. *Eur J Biochem* 260:785-793.
502 34. Choi SY, Fogelgren B, Zuo, Z, Juang L, McKenna S, Lingappa VR, Lipschutz JH (2012).
503 Exocyst Sec10 is involved in basolateral protein translation and translocation in the
504 endoplasmic reticulum. *Nepron Exp Nephrol* 120:e133-e139.
505 35. Washiyama M, Koizumi N, Fujii M, Watanabe Y (2014). Sec61ß regulates barrier functions of
506 tight junctions through expression of claudin-4 in MDCK cells. *Biol Pharm Bull* 37:979-986.
507 36. Valcarcel R, Weber U, Jackson DB, Benes V, Ansorge W, Bohmann D, Mlodzik M (1999).
508 Sec61beta, a subunit of the protein translocation cannel, is required during Drosophila
509 development. *J Cell Sci* 112:4389-96.
510 37. Kannan N, Neuwald AF (2005). Evolutionary constraints associated with functional specificity
511 of the CMGC protein kinases MAPK, CDK, GSK, SRPK, DYRK, and CK2alpha. *Protein Sci*
512 13:2059-77.
513 38. Finke K, Plath K, Panzner S, Prehn S, Rapoport TA, Hartmann E, Sommer T (1996). A second
514 trimeric complex containing homologs of the Sec61p complex functions in protein transport
515 across the ER membrane of *S. cerevisiae*. *EMBO J* 15:1482-94.

516 39. Barbieri G, Simon J, Lupusella CR, Pereira F, Elia F, Meyer H, Schuldiner M, Hanes SD,
517 Nguyen D, Helms V, Römisch K (2023) Sbh1/Sec61ß promotes ER translocation of proteins
518 with suboptimal targeting sequences and is fine-tuned by phosphorylation. biorxiv
519 **doi:** https://doi.org/10.1101/2022.05.18.492448
520 40. Wright, C. M., Fewell, S. W., Sullivan, M. L., Pipas, J. M., Watkins, S. C., and Brodsky, J. L.
521 (2007) The Hsp40 molecular chaperone Ydj1p, along with the protein kinase C pathway,
522 affects cell-wall integrity in the yeast *Saccharomyces cerevisiae*. *Genetics* **175**, 1649-1664
523 41. Roncero C, Valdivieso MH, Ribas JC, Durán (1988). Isolation and characterization of
524 *Saccharomyces cerevisiae* mutants resistant to Calcofluor white. J Bacteriol 170:1950-54.
525 42. Lesage G, Bussey H (2006). Cell wall assembly in *Saccharomyces cerevisiae*. Microbiol Mol
526 Biol Reviews 70:317-343.
527 43. Ziska A, Tatzelt J, Dudek J, Paton AW, Paton JC, Zimmermann R, Haßdenteufel S (2019). The
528 signal peptide plus a cluster of positive charges in prion protein dictate chaperone-mediated
529 Sec61-channel gating. *Biol Open* 8(3). pii:bio040691.
530 44. Itskanov S, Park E (2019). Structure of the posttranslational Sec protein translocation channel
531 complex from yeast. *Science* 363:84-87.
532 45. Mades A, Gotthardt K, Awe K, Stieler J, Döring T, Füser S, Prange R (2012). Role of human
533 Sec63 in modulating the steady-state levels of multi-spanning membrane proteins. *PLoS One*
534 7:e49243.
535 46. Jung SJ, Kim JE, Reithinger JH, Kim H (2014). The Sec62-Sec63 translocon facilitates
536 translocation of the C-terminus of membrane proteins. *J Cell Sci* 127:4270-78.
537 47. Vembar SS, Jonikas MC, Hendershot LM, Weissman JS, Brodsky JL (2010). J domain co-
538 chaperone specificity defines the role of BiP during protein translocation. J Biol Chem
539 285:22484-94.

540 48. Matlack KE, Misselwitz B, Plath K, Rapoport TA (1999). BiP acts as a molecular ratchet
541 during posttranslational transport of prepro-alpha factor across the ER membrane. *Cell* 97:
542 553-564.
543 49. Allen WJ, Collinson I, Römisch K (2019). Post-translational protein transport by the Sec
544 complex. Trends Biochem Sci pii:S0968-0004(19)30056-8.
545 50. Hegde RS, Bernstein HD (2006). The surprising complexity of signal sequences. *Trends*
546 *Biochem Sci* 31:563-571.
547 51. Banks, I. R., Specht, C. A., Donlin, M. J., Gerik, K. J., Levitz, S. M., and Lodge, J. K. (2005) A
548 chitin synthase and its regulator protein are critical for chitosan production and growth of the
549 fungal pathogen *Cryptococcus neoformans*. *Eukaryot Cell* **4**, 1902-1912
550 52. Baker, L. G., Specht, C. A., Donlin, M. J., and Lodge, J. K. (2007) Chitosan, the deacetylated
551 form of chitin, is necessary for cell wall integrity in *Cryptococcus neoformans*. *Eukaryot Cell* **6**,
552 855-867
553 53. Liu OW, Chun CD, Chow ED, Chen C, Madhani HD, Noble SM (2008). Systematic genetic
554 analysis of virulence in the fungal pathogen *Cryptococcus neoformans*. Cell 135:174-188.
555 54. Chen, Y., Toffaletti, D. L., Tenor, J. L., Litvintseva, A. P., Fang, C., Mitchell, T. G.,
556 McDonald, T. R., Nielsen, K., Boulware, D. R., Bicanic, T., and Perfect, J. R. (2014) The
557 *Cryptococcus neoformans* transcriptome at the site of human meningitis. *MBio* **5**, e01087-
558 01013
559 55. Liu OW, Kelly MJ, Chow ED, Madhani HD (2007). Parallel beta-helix proteins required for
560 accurate capsule polysaccharide synthesis and virulence in the yeast *Cryptococcus neoformans*.
561 *Eukaryot Cell* 6:630-640.
562 56. Kumar P, Heiss C, Santiago-Tirado FH, Black I, Azadi P, Doering TL (2014). Pbx proteins in
563 *Cryptococcus neoformans* cell wall remodeling and capsule assembly. *Eukaryot Cell*
564 13:560-571.

565 57. Gilbert NM, Donlin MJ, Gerik KJ, Specht CA, Djordjevic JT, Wilson CF, Sorrell TC, Lodge
566 JK (2010). *KRE* genes are required for beta-1,6-glucan synthesis, maintenance of capsule
567 architecture and cell wall protein anchoring in *Cryptococcus neoformans*. *Mol Microbiol*
568 76:517-534.
569 58. Chang YC, Kwon-Chung KJ (1998). Isolation of the third capsule-associated gene, *CAP60*,
570 required for virulence in *Cryptococcus neoformans*. *Infect Immun* 66:2230-2236.
571 59. Vu K, Tham R, Uhrig JP, Thompson GR 3rd, Na Pombejra S, Jamklang M, Bautos JM, Gelli A
572 (2014). Invasion of the central nervous system by *Cryptococcus neoformans* requires a
573 secreted fungal metalloprotease. *MBio* 5: e01101-01114.
574 60. Monod M, Capoccia S, Lechenne B, Zaugg C, Holdom M, Jousson O (2002). Secreted
575 proteases from pathogenic fungi. *Int J Med Microbiol* 292:405-419.
576 61. Maier EJ, Haynes BC, Gish SR, Wang ZA, Skowyra ML, Marulli AL, Doering TL, Brent MR
577 (2015). Model-driven mapping of transcriptional networks reveals the circuitry and dynamics
578 of virulence regulation. *Genome Res* 25: 690-700.
579 62. Wei YY, Liang S, Zhang YR, Lu JP, Lin FC, Liu XH (2020). MoSec61ß, the beta subunit of
580 Sec61, is involved in fungal development and pathogenicity, plant immunity, and ER-phagy in
581 Magnaporthe oryzae. *Virulence* 11:1685-1700.
582 63. Skowyra ML, Doering TL (2012). RNA interference in *Cryptococcus neoformans*. *Methods*
583 *Mol Biol* 845:165–86.
584 64. Gerik KJ, Donlin MJ, Soto CE, Banks AM, Banks IR, Maligie MA, Selitrennikoff CP, Lodge
585 JK (2005). Cell wall integrity is dependent on the *PKC1* signal transduction pathway in
586 *Cryptococcus neoformans*. *Mol Microbiol* 58:393–408.
587 65. Geddes JM, Caza M, Croll D, Stoynov N, Foster LJ, Kronstad JW (2016). Analysis of the
588 protein kinase A-regulated proteome of *C. neoformans* identifies a role for the ubiquitin-
589 proteasome pathway in capsule formation. MBio 7:e01862-15.

590 66. Ball B, Geddes-McAlister J (2019). Quantitative Proteomic Profiling of *Cryptococcus*
591 *neoformans*. *Curr Protocols Microbiology* 55:e94.
592 67. Santiago-Tirado FH, Peng T, Yang M, Hang HC, Doering TL (2015). A single protein S-acyl
593 transferase acts through diverse substrates to determine cryptococcal morphology, stress
594 tolerance, and pathogenic outcome. *PLoS Pathog* 11(5):e1004908.
595 68. Cadieux B, Lian T, Hu G, Wang J, Biondo C, Teti G, Liu V, Murphy M, Creagh, AL, and
596 Kronstad JW (2013). The Mannoprotein Cig1 supports iron acquisition from heme and
597 virulence in the pathogenic fungus *Cryptococcus neoformans*. *J Infect Dis* 207:1339-1347.

598

599 **TABLE 1**

Gene ID	Gene name	Protein function	SP or TM	WT/*sbh1Δ* proteomics [log2-fold]	Virulence citations	24 h/0 h RNA-seq
CNAG_00150		serine endoptidase, cell wall	SP1-23	5.24	53	1.68
CNAG_01653	*CIG1*	cytokine-inducing glycoprotein	SP1-19	4.00	68	385.34
CNAG_01172	*PBX1*	beta-helix containing protein	SP1-18	3.68	55,53,56	0.78
CNAG_04735	*MPR1*	extracellular metalloproteinase (Mep1)	SP1-19	3.44	53, 59	122.79
CNAG_00897	*SKN1*	glucosidase	TM134-58	3.04	57	3.43
CNAG_02030		glyoxal oxidase	SP1-21	2.79	53	0.97
CNAG_00600	*CAP60*	capsule-associated protein	SP1-33	2.65	58	1.97
CNAG_01331			SP1-18	2.62	53	13.45

600

601 **Table 1. Sbh1-dependent proteins involved in cryptococcal virulence.**

602 These proteins meet the following criteria: their expression in 37D5 was at least two-fold higher in
603 WT compared to *sbh1Δ* cells; they contain an SP or TM domain; and they are required for normal
604 *C. neoformans* virulence in mouse infections. Note that this is likely a subset of such proteins, as
605 most cryptococcal proteins have not been tested for roles in virulence; other candidates that meet
606 the first two criteria are listed in Supplementary Table 1. Proteomics results are shown as the ratio
607 of expression in WT versus *sbh1Δ* cells in 37D5. RNA-seq results are shown as the ratio of gene
608 expression at 24 h versus 0 h in 37D5 (61). Expression of a subset of these genes (CNAG_04735,
609 CNAG_02030, CNAG_00897) was measured by qPCR; these studies confirmed that it is not
610 affected by loss of *SBH1* (Supplementary Figure 3).

611

612 **FIGURE LEGENDS**

613 **FIGURE 1: Sbh1 is required for cell wall integrity in *S. cerevisiae*. A)** Structure of the Sec61
614 channel of *S. cerevisiae* (modified from 12; PDB 6ND1). The N-terminal half of Sec61 is shown in
615 blue, C-terminal half in green, Sss1 in grey, and Sbh1 in magenta. The intrinsically unstructured N-
616 terminal 38 amino acids of Sbh1 that were not visible in the cryo-EM structure were drawn in by
617 hand. P, phosphorylation sites; dashed lines, position of the ER membrane; arrow, direction of
618 protein transport. **B)** Alignment of the poorly conserved N-termini of Sbh1 proteins from *S.*
619 *cerevisiae* (Sbh1, Sbh2) and the following pathogenic fungi: Cryn *Cryptococcus neoformans*, Sjap
620 *Schizosaccharomyces japonicus*, Hcap *Histoplasma capsulatum*, Bder *Blastomyces dermatitidis*,
621 Cpos *Coccidioides posadasii*, Afum *Aspergillus fumigatus*, Anig *Aspergillus niger*, Bfuc
622 *Botryotinia fuckeliana*, Sbra *Sporothrix brasiliensis*. Except for Sbh2, only regions containing S or
623 T residues with flanking prolines (pink) are shown. The conserved proline-flanked T5 in *S.*
624 *cerevisiae* Sbh1 is indicated by an asterisk; other confirmed phosphorylation sites in *S. cerevisiae*
625 Sbh1 are shown in grey; and the PKA site in *C. neoformans* Sbh1 is in blue. *Schizosaccharomyces*
626 *cryophilus*, *Schizosaccharomyces octoporus*, *Candida albicans*, *Schizosaccharomyces pombe*,
627 *Kluyveromyces lactis*, *Yarrowia lipolytica*, *Pichia pastoris*, and *Hansenula polymorpha* Sbh1
628 proteins were also screened, but do not contained potential proline-flanked phosphorylation sites.
629 For full alignments of all Sbh1 protein sequences see Supplementary Figure 1. **C)** Wildtype *SBH1*
630 *SBH2 S. cerevisiae* and the indicated mutants were grown on YPD plates at the indicated
631 temperatures for 3 days. **D)** The Δ*sbh1*Δ*sbh2 S. cerevisiae* strain was transformed with pRS415
632 without an insert *(*vector), wildtype *SBH1*, or the indicated phosphorylation site mutants and grown
633 on SC without leucine containing 10 µg/ml calcofluor white at 30°C. A Δ*kre6* mutant which is
634 unable to grow on calcofluor white and its isogenic wildtype were included as controls. Note that
635 these are in a different strain background compared to the *SBH1* strain. **E)** The indicated strains,
636 including the untransformed Δ*sbh1*Δ*sbh2 S. cerevisiae* strain (Δ*sbh1/2*), were grown to early

637 exponential phase and cell-wall proteins were extracted by high pH/DTT, resolved by SDS-PAGE
638 (size range shown is roughly 10-150 kD), and visualized by Coomassie staining.
639
640 **FIGURE 2: Sbh1 is required for cell wall integrity at high temperature in *C.neoformans*.**
641 **A)** Serial 10-fold dilutions of wild-type (KN99) and Δ*sbh1* cells were grown at the temperatures
642 shown on YPD alone or containing 1 mg/ml calcofluor white (CFW) or 0.02% SDS (SDS). **B)**
643 Wild type (KN99) or *sbh1*Δ mutant cells were transformed with vector alone (vec) or plasmids
644 encoding HA-tagged Sbh1 (SBH1), or Sbh1 with mutations in the indicated phosphorylation sites
645 and then diluted as in panel A and grown at the indicated conditions. **C)** Cells of the strains
646 indicated were treated with lysing enzymes (see Methods) for the times shown and then assessed
647 for % lysis with two-way ANOVA with mixed-effects analysis. * indicates $P<0.05$, # indicates
648 $P=0.25$. **D)** The indicated strains were grown as above in the presence of 1 mM H_2O_2 or 1mM
649 $NaNO_2$ on YNB (pH 5) at 37°C. All experiments are representative of at least three biological
650 replicate studies.
651
652 **FIGURE 3: *C. neoformans* Sbh1 is required for the induction of secretory and**
653 **transmembrane proteins in conditions that mimic the host.** Proteomic analysis of wildtype and
654 *sbh1*Δ *C. neoformans* grown in YPD at 30°C or in 37D5. Samples were analyzed in quadruplicate.
655 Gene IDs of known virulence factors are indicated by asterisks.
656
657 **FIGURE 4: Secretory and transmembrane proteins that require Sbh1 for induction contain**
658 **specific ER-targeting sequences. A)** Characterization of Sbh1-dependent transmembrane
659 domains. Top, schematic of a typical transmembrane domain (TMD) with features specific for
660 Sbh1-dependent TMDs highlighted in red. Hydrophobicity (left) and charges within 10 amino acids
661 of TMDs (right) were analyzed for TMDs of Sbh1-dependently induced proteins (candidates, red)
662 compared to all transmembrane proteins in the *C. neoformans* proteome (black). **B**)

663 Characterization of Sbh1-dependent signal peptides. The schematic on top shows a typical signal
664 peptide (SP) with features specific for Sbh1-dependent SPs highlighted in red. Black triangle:
665 signal peptidase cleavage site. SPs of Sbh1-dependently induced secretory proteins (red) were
666 analyzed for N-region charge, H-region hydrophobicity and length, and C-region polarity and
667 compared to all signal peptides in the *C. neoformans* proteome (black). The only difference found
668 was in C-region polarity, shown in the graph. **C)** Model for Sbh1 function in *C. neoformans*. Under
669 rich medium conditions, proteins with Sbh1-dependent ER targeting sequences (magenta) play only
670 a minor role for vegetative growth (left), and most proteins imported into the ER have Sbh1-
671 independent targeting sequences (shaded grey). During infection (right), however, Sbh1-dependent
672 ER import (magenta) becomes essential.
673
674 **FIGURE 5: The *C. neoformans sbh1*Δ mutant is defective in growth in conditions that mimic**
675 **the host or within host cells and is avirulent in mouse infection.** (A) Fungi of the indicated
676 strains were incubated in tissue culture medium (5% CO_2, 37 °C) for 1, 18, or 30 h and then plated
677 on YPD for enumeration of colony-forming units (CFU; shown normalized to the 1 h CFU value).
678 Shown are mean and SEM values from 4 independent experiments. (B) Cells were incubated for 1
679 h with differentiated THP-1 cells (MOI = 1), during which time fungi were engulfed by the host
680 cells. Samples were then vigorously washed to remove free cryptococci and host cells were lysed to
681 measure CFU either immediately or after 30 h of incubation. % change was calculated as [(Final
682 CFU – Initial CFU) / (Initial CFU)] x 100]. Shown are mean and SEM values from 2 independent
683 experiments. For (A) and (B), * indicates $p < 0.05$ for *sbh1*Δ compared to KN99. (C, D) Total
684 fungal burden at 14 days post-infection with the indicated strains, measured in lung (C) and brain
685 (D). Each symbol represents colony forming units (CFU) for one mouse; mean and standard
686 deviation are also shown. Dotted line, original inoculum. (E) Mouse survival after intranasal
687 infection with $5x10^4$ cells of KN99 wildtype (solid line), *sbh1*Δ (dashed line) or
688 *sbh1*Δ complemented with wildtype *SBH1* (dotted line). (F) Weight (mean and SD) of the mice

689 from Panel E over time after infection. Any mouse that decreased to less than 80% of its initial
690 weight (indicated by dashed lines) was humanely sacrificed and considered not to survive the
691 infection.
692
693 **SUPPLEMENTARY INFORMATION**
694
695 **SUPPLEMENTAL METHODS (word doc)**
696
697 **TABLE S1 (Excel file): Protein expression analysis in KN99 wild-type and *sbh1*Δ *C.***
698 ***neoformans* grown in YPD at 30°C or DMEM at 37°C and 5% CO_2.**
699 Proteins are ordered by degree of Sbh1-dependence (log_2 of wild-type/*sbh1*Δ LFQ intensity).
700 Where present, ER targeting sequences are indicated by amino acid numbers. SP, signal peptides;
701 SA, uncleaved signal anchors; TM, first transmembrane domain. Ambiguous predictions due to
702 limited hydrophobicity (TM) or suboptimal signal peptide parameters (SP) are indicated by '?'.
703
704 **TABLE S2 (word doc): Signal peptides and transmembrane domains of proteins induced in**
705 **DMEM in KN99 wildtype *C. neoformans*.** Amino acid sequences of TM domains, signal
706 peptides, and signal anchors are shown including the flanking 10 amino acids on either side for TM
707 or the first 10 amino acids of the mature domains for SP. Positively charged amino acid residues
708 are highlighted in red.
709
710 **SUPPLEMENTARY FIGURE 1: Alignments of full Sbh1 amino acid sequences.** Protein
711 sequences were extracted from Uniprot and aligned using Clustal Omega. (A) Sbh1 orthologues
712 with N-terminal, proline-flanked S or T. Sbh1 = *S. cerevisiae*, proline-flanked N-terminal
713 phosphorylation sites highlighted in yellow; Cryn *Cryptococcus neoformans*, Sjap
714 *Schizosaccharomyces japonicus*, Hcap *Histoplasma capsulatum*, Bder *Blastomyces dermatitidis*,

715 Cpos *Coccidioides posadasii*, Afum *Aspergillus fumigatus*, Anig *Aspergillus niger*, Bfuc
716 *Botryotinia fuckeliana*, Sbra *Sporothrix brasiliensis*. (B) Sbh1 orthologues without N-terminal,
717 proline-flanked S or T. *S. cerevisiae* Sbh1 is shown for comparison; Sbh2 = *S. cerevisiae* paralogue
718 without N-terminal, proline-flanked S or T; Scry, *Schizosaccharomyces cryophilus*, Soct
719 *Schizosaccharomyces octoporus*, Cal *Candida albicans*, Spom *Schizosaccharomyces pombe*, Klac
720 *Kluyveromyces lactis*, Ylip *Yarrowia lipolytica*, Ppas *Pichia pastoris*, Hpol *Hansenula*
721 *polymorpha.*
722
723 **SUPPLEMENTARY FIGURE 2: Expression of wild type and phosphorylation mutants of**
724 **Sbh1.** Shown is an anti-HA immunoblot of wildtype or *sbh1*Δ cryptococcal cells expressing either
725 vector alone (vec) or the indicated HA-tagged proteins. 20 ug of lysate were resolved on a 4 – 20%
726 gradient gel and transferred onto PDVF membrane, which was stained with Ponceau S. This blot is
727 representative of three independent experiments. The numbers and lines on the left represent the
728 protein ladder. The Sbh1-5XHA protein is ~16kDa.
729
730 **SUPPLEMENTARY FIGURE 3: qRT-PCR analysis of selected genes in WT, *sbh1* mutant,**
731 **and complemented strains grown in conditions that mimic the host** (DMEM, 37°C, 5% CO_2,
732 24 h). For each gene indicated, the plot shows mean and standard deviation of results from three
733 biological replicates, each done in technical triplicate and normalized to *ACT1* expression. There
734 were no significant differences in gene expression for any pairwise comparison between strains (all
735 $P > 0.2$ by unpaired T-test).

Figure 1

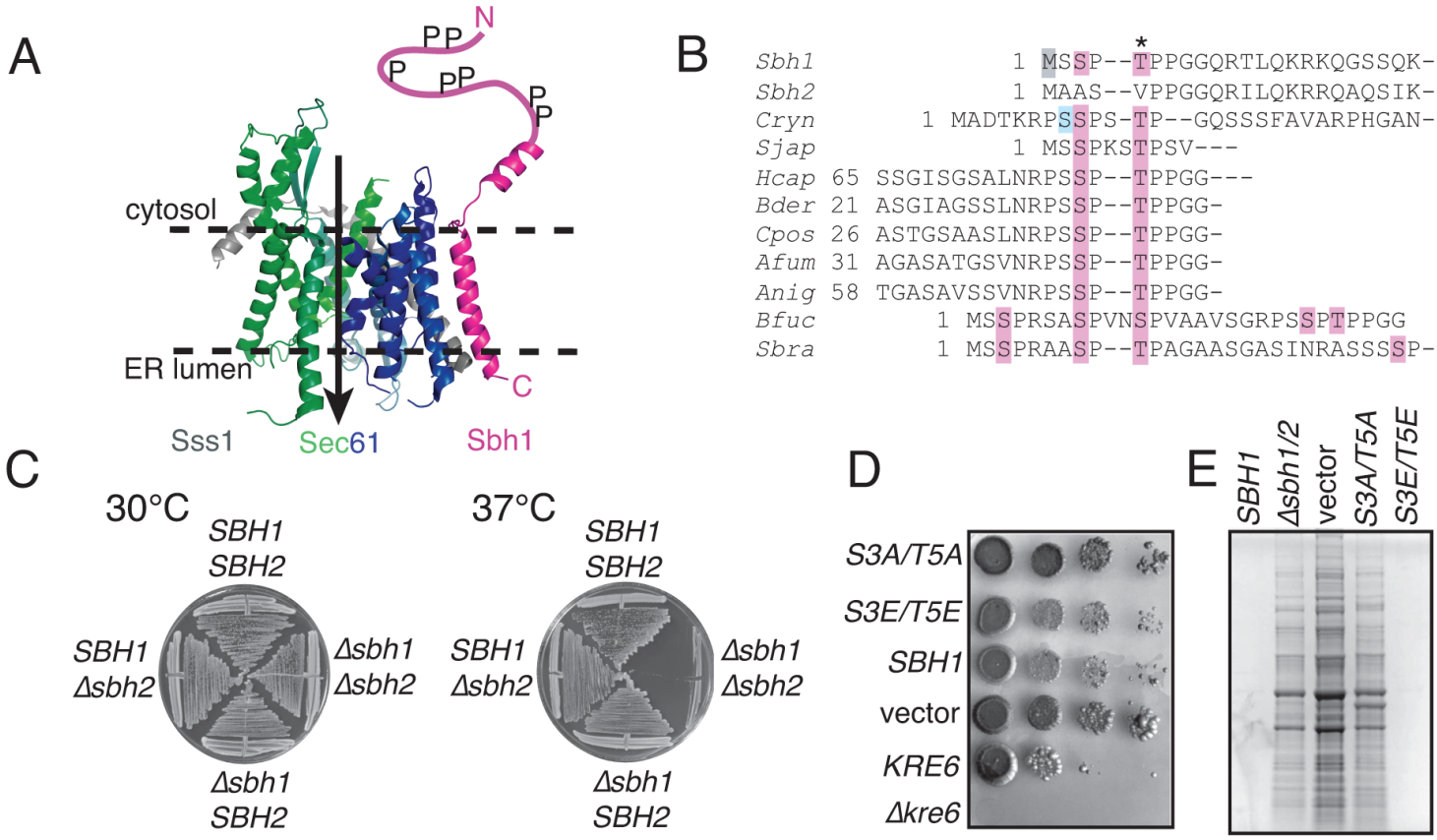
A
N
P P
P
P P
P
P
cytosol
ER lumen
C
Sss1
Sec61
Sbh1
B
*
Sbh1 1 MSSP--TPPGGQRTLQKRKQGSSQK-
Sbh2 1 MAAS--VPPGGQRILQKRRQAQSIK-
Cryn 1 MADTKRPSSPS-TP--GQSSSFAVARPHGAN-
Sjap 1 MSSPKSTPSV---
Hcap 65 SSGISGSALNRPSSP--TPPGG---
Bder 21 ASGIAGSSLNRPSSP--TPPGG-
Cpos 26 ASTGSAASLNRPSSP--TPPGG-
Afum 31 AGASATGSVNRPSSP--TPPGG-
Anig 58 TGASAVSSVNRPSSP--TPPGG-
Bfuc 1 MSSPRSASPVNSPVAAVSGRPSSPTPPGG
Sbra 1 MSSPRAASP--TPAGAASGASINRASSSSP-
C
30°C
SBH1
SBH2
SBH1
Δsbh2
Δsbh1
Δsbh2
Δsbh1
SBH2
37°C
SBH1
SBH2
SBH1
Δsbh2
Δsbh1
Δsbh2
Δsbh1
SBH2
D
S3A/T5A
S3E/T5E
SBH1
vector
KRE6
Δkre6
E
SBH1
Δsbh1/2
vector
S3A/T5A
S3E/T5E

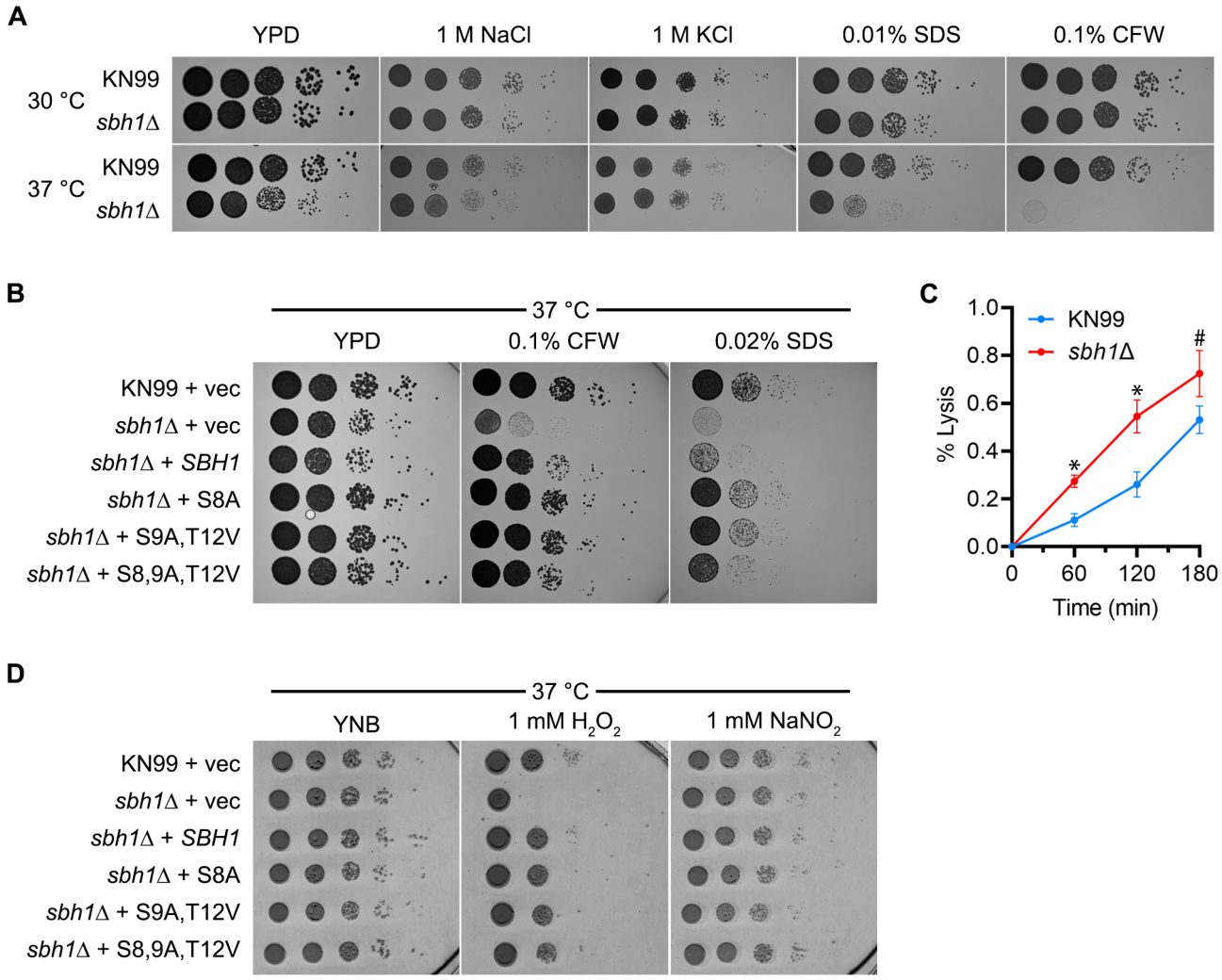
A
YPD
1 M NaCl
1 M KCl
0.01% SDS
0.1% CFW
30 °C
KN99
sbh1Δ
37 °C
KN99
sbh1Δ
B
37 °C
YPD
0.1% CFW
0.02% SDS
KN99 + vec
sbh1Δ + vec
sbh1Δ + SBH1
sbh1Δ + S8A
sbh1Δ + S9A,T12V
sbh1Δ + S8,9A,T12V
C
KN99
sbh1Δ
% Lysis
1.0
0.8
0.6
0.4
0.2
0.0
0
60
120
180
Time (min)
*
*
#
D
37 °C
YNB
1 mM H2O2
1 mM NaNO2
KN99 + vec
sbh1Δ + vec
sbh1Δ + SBH1
sbh1Δ + S8A
sbh1Δ + S9A,T12V
sbh1Δ + S8,9A,T12V

Figure 3

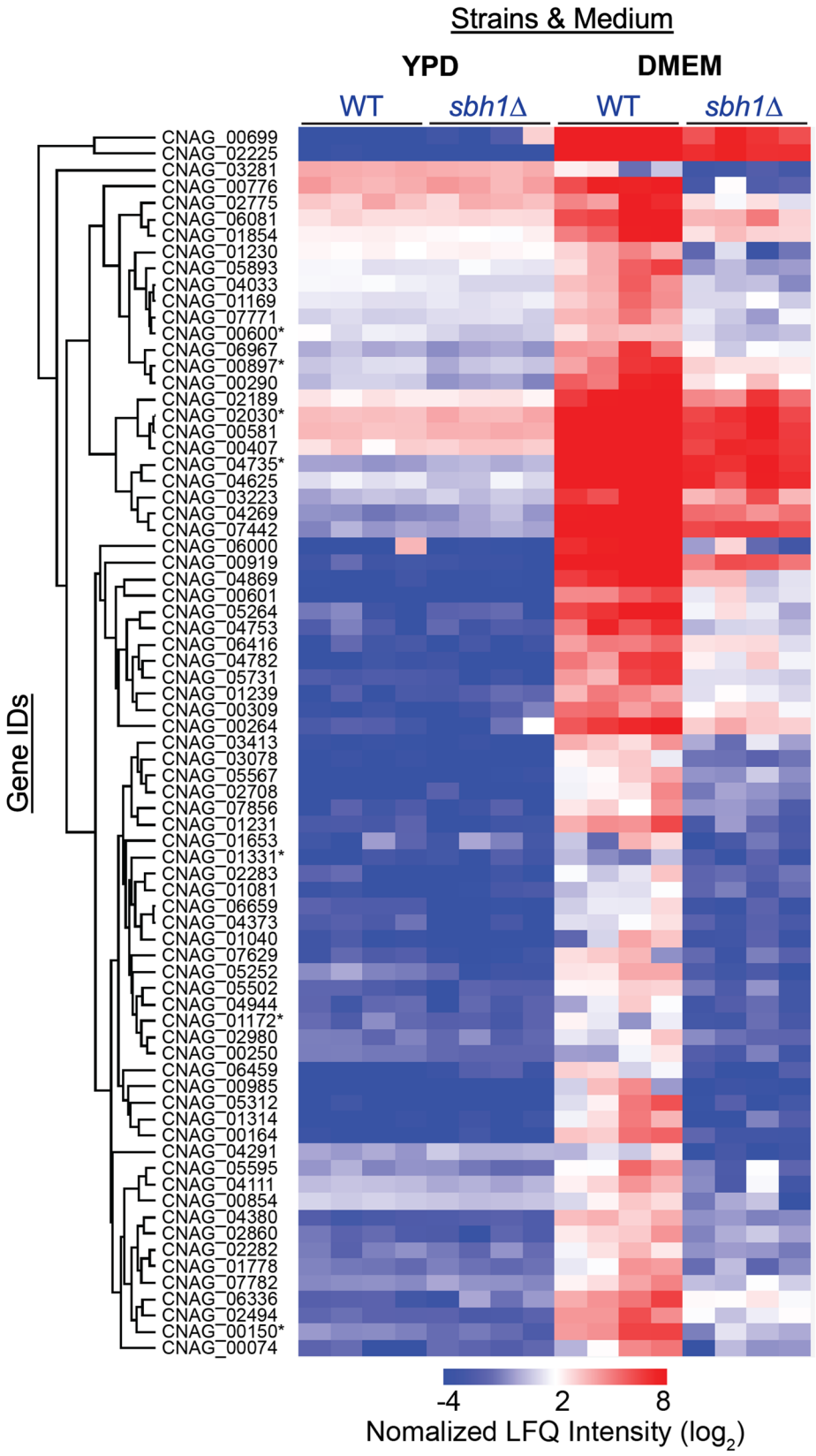
Strains & Medium
YPD
DMEM
WT
sbh1Δ
WT
sbh1Δ
Gene IDs
CNAG_00699
CNAG_02225
CNAG_03281
CNAG_00776
CNAG_02775
CNAG_06081
CNAG_01854
CNAG_01230
CNAG_05893
CNAG_04033
CNAG_01169
CNAG_07771
CNAG_00600*
CNAG_06967
CNAG_00897*
CNAG_00290
CNAG_02189
CNAG_02030*
CNAG_00581
CNAG_00407
CNAG_04735*
CNAG_04625
CNAG_03223
CNAG_04269
CNAG_07442
CNAG_06000
CNAG_00919
CNAG_04869
CNAG_00601
CNAG_05264
CNAG_04753
CNAG_06416
CNAG_04782
CNAG_05731
CNAG_01239
CNAG_00309
CNAG_00264
CNAG_03413
CNAG_03078
CNAG_05567
CNAG_02708
CNAG_07856
CNAG_01231
CNAG_01653
CNAG_01331*
CNAG_02283
CNAG_01081
CNAG_06659
CNAG_04373
CNAG_01040
CNAG_07629
CNAG_05252
CNAG_05502
CNAG_04944
CNAG_01172*
CNAG_02980
CNAG_00250
CNAG_06459
CNAG_00985
CNAG_05312
CNAG_01314
CNAG_00164
CNAG_04291
CNAG_05595
CNAG_04111
CNAG_00854
CNAG_04380
CNAG_02860
CNAG_02282
CNAG_01778
CNAG_07782
CNAG_06336
CNAG_02494
CNAG_00150*
CNAG_00074
-4
2
8
Nomalized LFQ Intensity (log2)

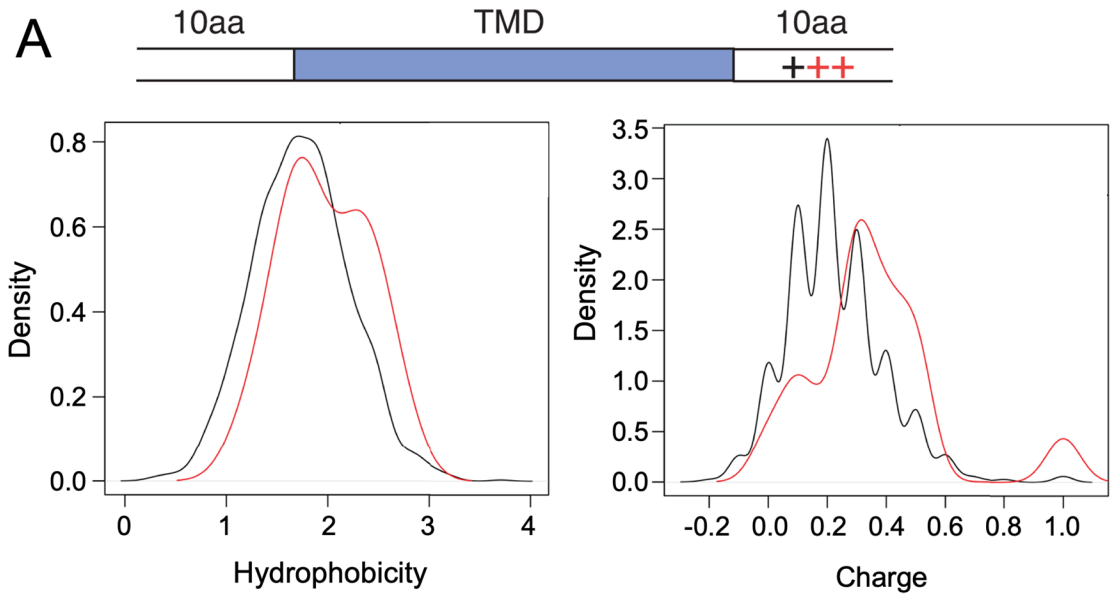
A
10aa
TMD
10aa
+++
Density
0.0
0.2
0.4
0.6
0.8
0
1
2
3
4
Hydrophobicity
Density
0.0
0.5
1.0
1.5
2.0
2.5
3.0
3.5
-0.2
0.0
0.2
0.4
0.6
0.8
1.0
Charge

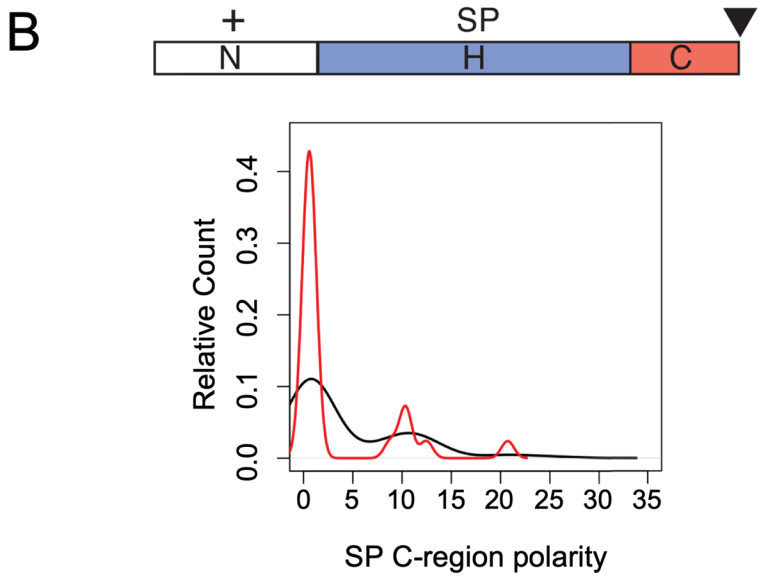
B
+
SP
N
H
C
Relative Count
0.0
0.1
0.2
0.3
0.4
0
5
10
15
20
25
30
35
SP C-region polarity

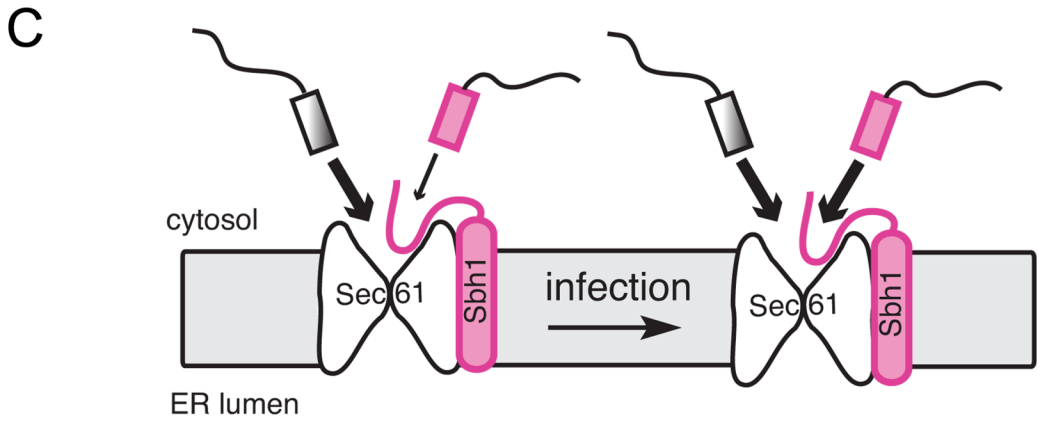
C
cytosol
Sec 61
Sbh1
infection
Sec 61
Sbh1
ER lumen

Figure 5

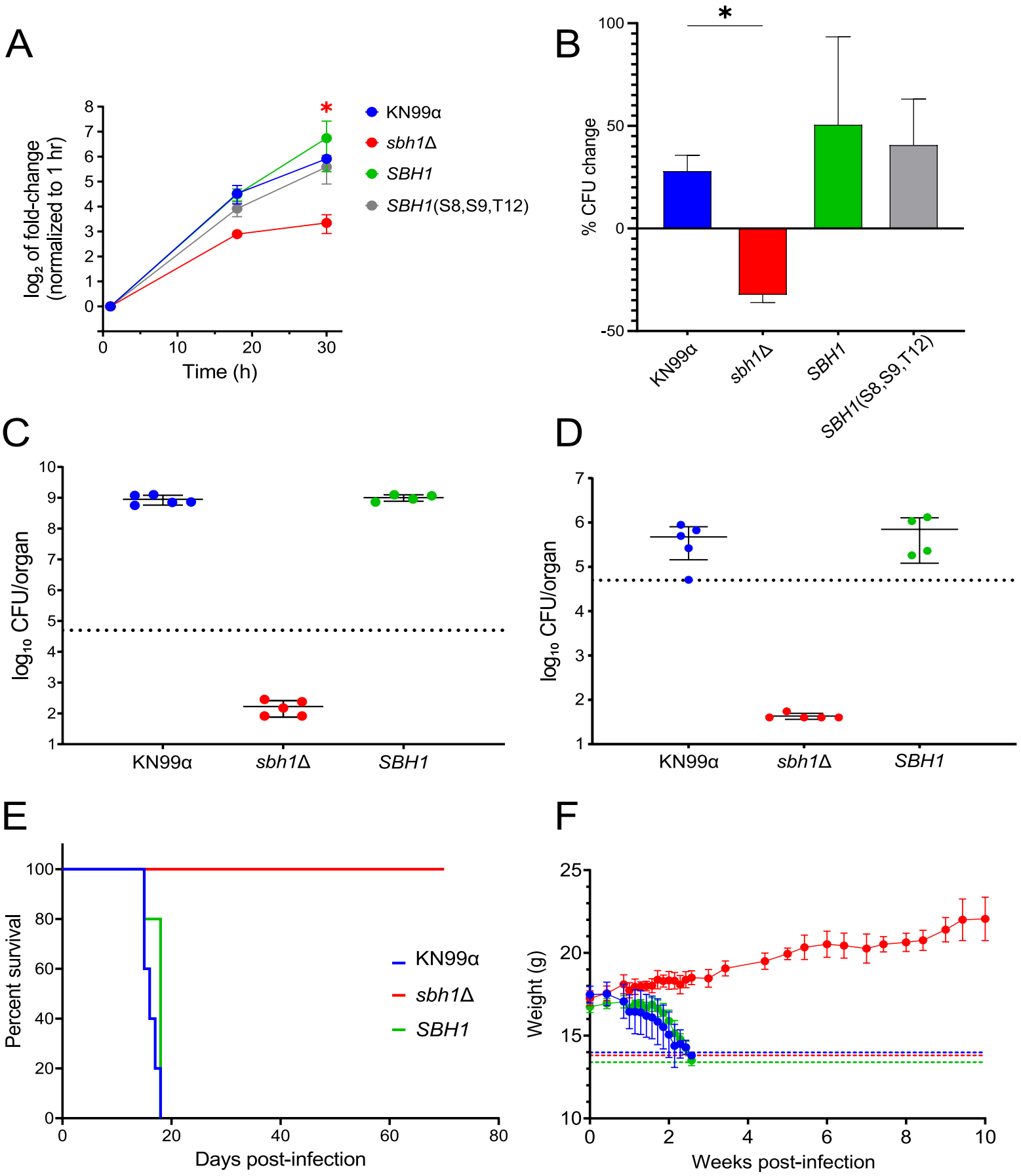
A
log2 of fold-change (normalized to 1 hr)
Time (h)
KN99α
sbh1Δ
SBH1
SBH1(S8,S9,T12)
*
B
% CFU change
KN99α
sbh1Δ
SBH1
SBH1(S8,S9,T12)
*
C
log10 CFU/organ
KN99α
sbh1Δ
SBH1
D
log10 CFU/organ
KN99α
sbh1Δ
SBH1
E
Percent survival
Days post-infection
KN99α
sbh1Δ
SBH1
F
Weight (g)
Weeks post-infection

A

```
CLUSTAL O(1.2.4) multiple sequence alignment


Sbh1      ------------------------------------------------------------  0
Cryn      ------------------------------------------------------------  0
Sjap      ------------------------------------------------------------  0
Cpos      ------------------------------------------MVSSSPLASGAESGNEAAKA  20
Afum      ---------------------------MHLLQ------ASARAASPLTSGAESGPDTKSS  27
Anig      ------------------------------------------------------------  0
Hcap      MPQGIYTTVDDERSLPGIREEFRSRNSSRLLQPILSFKTSPSNTMASGSGVESGAEGPKS  60
Bder      ---------------------------------------------MASGSGPDSGAEGAKS  16
Bfuc      --------------------------------------MSSPRSASPVNSPV---------  14
Sbra      --------------------------------------MSSPRAASPTPAGA---------  14


Sbh1      ----------------MSSPTPPGGQRTLQKRKQGSS---Q--KVAAS-----APKKNTN  34
Cryn      ----------MADTKRPSSPSTPGQSSSFAVARPHGANAVRRRAPAAARPSSTRSAGAGG  50
Sjap      -----MSSPKSTPSVKSSPGAAPGGPKSQIRR---RAAAEK-SKEGKALPAGPRAAGANG  51
Cpos      SNPTGASTGSAASLNRPSSPTPPGGPRTALRR---RAAADHKESVRNARPASTRAAGAGG  77
Afum      --GAGAGASATGSVNRPSSPTPPGGPRAALRR---RAAADHKESLRNARPSSTRAAGAGG  82
Anig      --------SAVSSVNRPSSPTPPGGPRAALRR---RAAADHKESLRNARPSSTRAAGAGG  49
Hcap      ASGASS-GISGSALNRPSSPTPPGGPRTAMRR---RAAADHKESIRNARPASTRSAGAGG  116
Bder      STGVAS-GIAGSSLNRPSSPTPPGGPRTAMRR---RAAADHKESIRNARPASTRSAGAGG  72
Bfuc      -----A-----AVSGRPSSPTPPGGPKTAIRR---RAAADQKDKVANARPSSTRAAGAGG  61
Sbra      -----ASGASINRASSSSPPPPPGGARTQIRR---RAAADQKEKVANSRPTSTRAAGAGG  66
                          *    **   :        :   :      :           .

Sbh1      SNNSILKIYSDE-ATGLRVDPLVVLFLAVGFIFSVVALHVISKVAGKLF-    82
Cryn      SSNTMLKLYTDSGEAGLKVDPFVVIVLSISFIASIFFLHITAKIIRAFTN    100
Sjap      STPTMLKLYTDE-TSGFKVDPVVVMVLSVGFIGSVFALHIIAKLMRKFSN    100
Cpos      SSGTMLKLYTDE-SPGLKVDPVVVLVLSLGFIFSVVGLHVIAKITRKFSS    126
Afum      SSGTMLKLYTDE-SPGLRVDPVVVLVLSLGFIFSVVGLHVIAKITRKFSS    131
Anig      SSGTMLKLYTDE-SPGLRVDPVVVLVLSLGFIFSVVGLHVIAKITRKFSA    98
Hcap      SSGTMLKLYTDE-SPGLKVDPVVVLVLSLGFIFSVVGLHVIAKISRKFA-    164
Bder      SSGTMLKLYTDE-SPGFKVDPVVVLVLSLGFIFSVVGLHVIAKITRKFSS    121
Bfuc      SSSTMLRLYTDE-SPGLKVDPVVVLVLSLVFIFSVVALHIIAKVTRKFSS    110
Sbra      SSSTMLRLYTDE-SPGLKVDPVVVLVLSLVFIFSVVALHIIAKITRRFSS    115
          *. ::*::*:*.   *::***.**:.*:: ** *:. **: :*:   :
```

B

```
Spom      MSSTKASGSVKNSAASAPGGPKSQIRRRAAVEKNTK-ESNSGPAGARAAGAPGSTPTLLK  59
Scry      MSSSKASGTVKNAGSSAPGGPKSQIRRRAAAEKTAK-DANTGPAGPRAAGAEGSTPTLLK  59
Soct      MSSSKASGTVKNAGSSAPGGPKSQIRRRAAAEKTAK-DSTTGPAGPRAAGADGSTPTLLK  59
Ylip      ----------MSTSAQVPGGPAAQMKRRNNAQRQEA-KASQRPTSTRSVGAGGSSSTMLK  49
Calb      ------MSASSSATNQAPGGLRSAVKRKTTQEKK-AQSSNATPLSTRSAGAGGSSSTMMK  53
Ppas      ------------MSTAIPGGQRTLAKRRAANLD----KKQDEPTSARSAGAGGSSSTMLK  44
Hpol      -------------MSSVPGGAKTLAKRKATQENKLKQQLQSQPTSTRAAGAGGSSSTMLK  47
Sbh1      -----------MSSPTPPGGQRTLQKRKQGSSQKVAA-SA-------PKKNTNSNNSILK  41
Sbh2      -----------MAASVPPGGQRILQKRRQAQSIKEKQ-AKQTPTSTRQAGYGGSSSSILK  48
Klac      ------------MDSSVPGGQRTLQKRRNAQLQKEKK-ANQTPASPRQAGFGGSSSSILK  47
                                 ***     :*:                       .*. ::*

Spom      LYTDEASGFKVDPVVVMVLSVGFIASVFLLHIVARILKKFASE   102
Scry      LYSDEATGFKVDPVVVMVLSVGFIASVFALHIVARILKNFASE   102
Soct      LYSDEATGFKVDPVVVMVLSVGFIASVFALHIVARVLKNFASE   102
Ylip      LYTDESQGLKVDPVVVMVLSLGFIFSVVALHILAKVSTKLLG-   91
Calb      LFTDEAQGLRVDPLVVLFLAVGFIFSVIILHVFAKITGKFTS-   95
Ppas      LYTDEAQGLKVDPLIVLVLAVGFIFSVIGLHVVAKLTGKLIN-   86
Hpol      IYTDESQGFKIDPLVVLVLAVSFIFSVVLLHVLAKLTGKFF--   88
Sbh1      IYSDEATGLRVDPLVVLFLAVGFIFSVVALHVISKVAGKLF--   82
Sbh2      LYTDEANGFRVDSLVVLFLSVGFIFSVIALHLLTKFTHII---   88
Klac      LYTDEANGLRVDPLVVLFLAVAFVFSVVALHVVAKVSGKIF--   88
          :::**: *:::* ::*:.*::.*: **. **:.::.   :
```

SUPPLEMENTARY FIGURE 1: Alignments of full Sbh1 amino acid sequences.

Protein sequences were extracted from Uniprot and aligned using Clustal Omega. (A) Sbh1 orthologues with N-terminal, proline-flanked S or T. Sbh1 = *S. cerevisiae*, proline-flanked N-terminal phosphorylation sites highlighted in yellow; Cryn *Cryptococcus neoformans*, Sjap *Schizosaccharomyces japonicus*, Hcap *Histoplasma capsulatum*, Bder *Blastomyces dermatitidis*, Cpos *Coccidioides posadasii*, Afum *Aspergillus fumigatus*, Anig *Aspergillus niger*, Bfuc *Botryotinia fuckeliana*, Sbra *Sporothrix brasiliensis*. (B) Sbh1 orthologues without N-terminal, proline-flanked S or T. *S. cerevisiae* Sbh1 is shown for comparison; Sbh2 = *S. cerevisiae* paralogue without N-terminal, proline-flanked S or T; Scry, *Schizosaccharomyces cryophilus*, Soct *Schizosaccharomyces octoporus*, Cal *Candida albicans*, Spom *Schizosaccharomyces pombe*, Klac *Kluyveromyces lactis*, Ylip *Yarrowia lipolytica*, Ppas *Pichia pastoris*, Hpol *Hansenula polymorpha.*

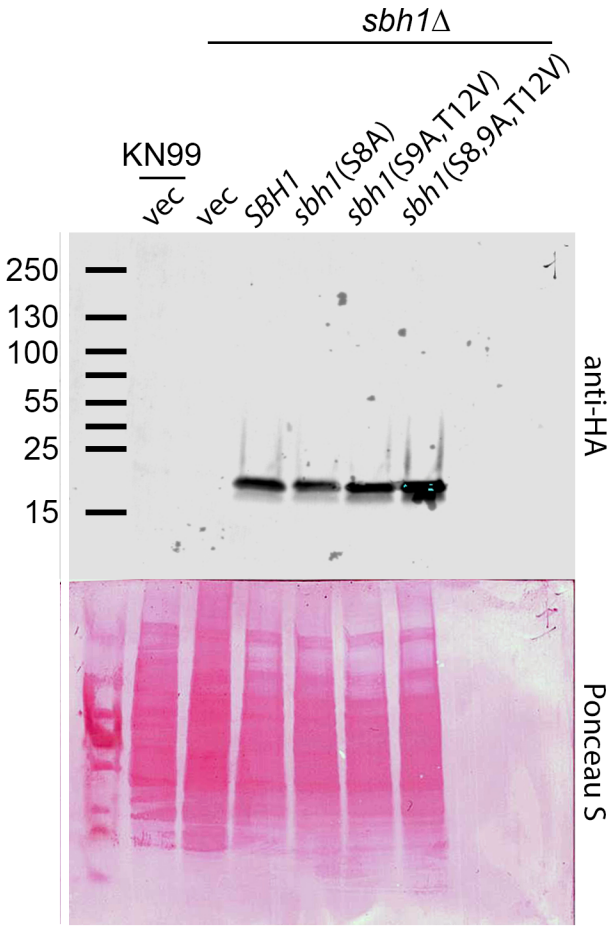

SUPPLEMENTARY FIGURE 2: Expression of wild type and phosphorylation mutants of Sbh1. Shown is an anti-HA immunoblot of wildtype or *sbh1*Δ cryptococcal cells expressing either vector alone (vec) or the indicated HA-tagged proteins. 20 ug of lysate were resolved on a 4 – 20% gradient gel and transferred onto PDVF membrane, which was stained with Ponceau S. This blot is representative of three independent experiments. The numbers and lines on the left represent the protein ladder. The Sbh1-5XHA protein is ~16kDa.

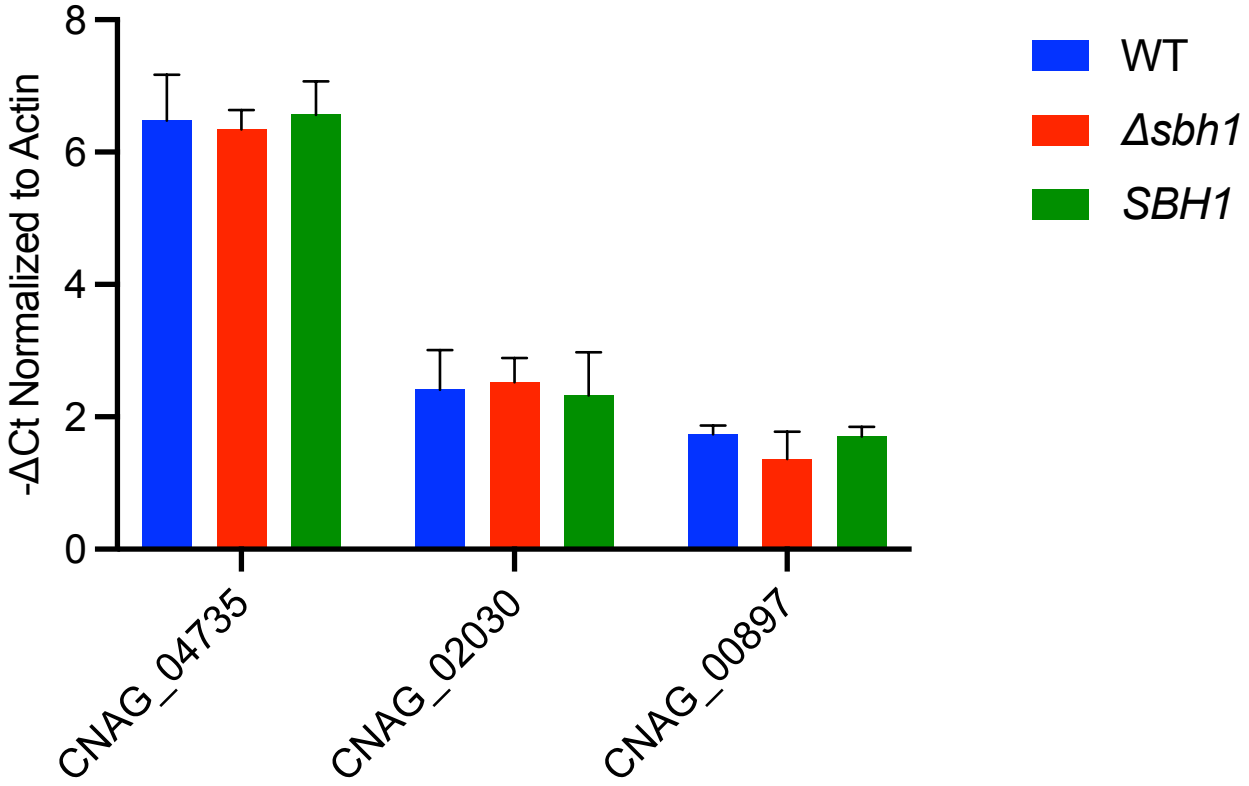

SUPPLEMENTARY FIGURE 3: qRT-PCR analysis of selected genes in WT, *sbh1* mutant, and complemented strains grown in host-like conditions (DMEM, 37°C, 5% CO_2, 24 h). For each gene indicated, the plot shows mean and standard deviation of results from three biological replicates, each done in technical triplicate and normalized to *ACT1* expression. There were no significant differences in gene expression for any pairwise comparison between strains (all $P > 0.2$ by unpaired T-test).

Santiago-Tirado *et al* **SUPPLEMENTAL METHODS**

S. cerevisiae strains and growth conditions

NY179 (*SBH1 SBH2 MAT* a *leu2-3,112 ura3-52*), H3223 (MAT a *KanMx::sbh1 leu2-3,112 ura3-52 GAL*$^+$), H3203 (MAT a *HphMx::sbh2 leu2-3,112 ura3-52 GAL*$^+$), and H3231 (MAT a *KanMx::sbh1 HphMx::sbh2 leu2-3,112 ura3-52 GAL*$^+$) were gifts from Jussi Jäntti and used to characterize Sbh1p phosphorylation sites (Toikkanen et al., 1996; Feng et al., 2007). *SBH1* cloned into pCR2.1-TOPO plasmid was kindly provided by Jussi Jäntti (Helsinki University, Finland). The QuickChange Site-Directed Mutagenesis Kit (Stratagene, UK) was used to introduce single or multiple base mutations in *SBH1.* Substitutions were verified by sequencing. Mutated *sbh1* was excised from pCR2.1-TOPO plasmids using EcoRV/BamHI, and subcloned into pRS415. For growth assays cells were grown on YPD or synthetic complete medium without leucine and with or without 10 µg/ml calcofluor white (Sigma) at 30°C or 37°C for 3 days.

S. cerevisiae cell wall extraction

Cells were grown in synthetic complete medium without leucine to early exponential phase and 10 OD_{600} harvested by centrifugation. Cells were resuspended in 100 µl 100 mM Tris-HCl, pH 9.4, 10 mM DTT, and incubated for 15 min at 37°C shaking at 800 rpm in a Thermomixer (Eppendorf). Samples were chilled for 1 min on ice, followed by sedimentation of the cells in a refrigerated Eppendorf centrifuge at maximal speed for 1 min. 90 µl of each supernatant were transferred to a new tube, carefully avoiding the pellet, and centrifuged again as above. 80 µl of each supernatant were transferred to a fresh tube and proteins precipitated by adding an equal volume of ice-cold 20 % trichloroacetic acid. Samples were mixed thoroughly and incubated on ice for 30 min. Proteins were sedimented by centrifugation at 4°C for 15 min and the pellets washed with ice-cold acetone, dried, and resuspended in 20 µl 2x SDS sample buffer by heating for 10 min to 95°C with agitation. Proteins were resolved on 4-14% Bis-Tris gels (NuPage) run in MOPS buffer and revealed by Coomassie staining.

C. neoformans strains and growth conditions

All strains used were in the *C. neoformans* serotype A strain KN99a background. The *sbh1*Δ deletion in this background used here was obtained from a library of partial gene deletions (generated by the Madhani group (Liu et al, 2008)) and available from the Fungal Genetics Stock Center at Kansas State University, Manhattan, KS) and confirmed by PCR. Fungal stocks were maintained at -80°C and grown at 30°C on yeast peptone dextrose (YPD) media with antibiotics as appropriate (100 µg/mL of nourseothricin (clonNAT, WERNER BioAgents, Germany) or 100 µg/mL G418 (Geneticin, Life Technologies, USA)).

SBH1 plasmid construction

For plasmid construction, the *SBH1* gene with its promoter and terminator sequences was amplified and cloned into ApaI/SpeI-digested pIBB103 (Skowyra and Doering, 2012). In parallel, a similar fragment lacking the terminator sequences and stop codon was amplified and cloned

into ApaI/SpeI-digested pFS5XHA (pIBB103 containing 5 HA epitopes followed by the *TRP1* terminator; this study). After both versions were confirmed to complement phenotypic defects, the tagged version was used for all subsequent analyses. This construct was used as template for mutagenesis of the N-terminal motifs of *SBH1* by using overlapping primers containing the codon changes and the forward and reverse primers used above. The resulting product was digested, cloned into pFS5XHA, and the whole insert sequenced to confirm mutations. These plasmids, together with an empty plasmid control, were electroporated into KN99a and the *sbh1*Δ strains as detailed below.

Electroporation of *C. neoformans*

Plasmid transformation was done by electroporation as described in (Skowyra and Doering, 2012). In brief, *Cryptococcus* cells patched on YPD agar plates with appropriate antibiotics were transferred into 5 ml of YPD liquid medium with antibiotic and cells were grown overnight at 30°C with shaking at 250 rpm. The overnight culture was diluted to an OD_{600} of 0.05 in 50 ml of fresh YPD medium (note that this OD_{600} value was measured in a multiplate reader and was not corrected for pathlength). After two doubling times the cells were transferred into conical tubes and sedimented, washed twice with cold dH_2O, and resuspended thoroughly in 50 ml cold EB buffer (10 mM Tris-HCl, pH 7.5, 1 mM $MgCl_2$, and 270 mM Sucrose) with 4 mM DTT. After incubation on ice for 15 min, the cells were pelleted, washed with 50 ml EB buffer without DTT, and resuspended in 1 ml EB buffer for counting. Cells were adjusted to 300 million cells per 100 µl, mixed with at least 1 µg of DNA (in no more than 1/10 of the total volume) and the mixture transferred into ice-cold 2 mm gap cuvettes. A Biorad electroporator was used with the following settings: V = 500v, R = infinity ohms, C = 25µF; the time constant should be 15 – 25 ms. Immediately after electroporation, 900 µl YPD without antibiotics was added and the cell suspension was transferred to a culture tube and incubated at 30°C for 3-4 h for recovery before various dilutions were spread on YPD plates with antibiotics to select transformants. Because of the heterogeneity in copy number associated with plasmids in *C. neoformans*, at least three independent colonies were picked and tested for each construct. All exhibited the same behaviors.

Phenotypic analysis

For stress plating, strains to be tested were grown overnight in YPD with antibiotic as appropriate, diluted to an OD_{600} of 0.05 in fresh YPD, and grown for two doublings. The cultures were then adjusted to 2 x 10^9 cells/ml, serially diluted (10-fold) and 5-µl aliquots were spotted onto the phenotyping plates described in the text. These plates did not include antibiotics because in combination with stressors they inhibit cell growth. Plates were incubated at 30°C and 37°C for 3-4 days.

The assay for sensitivity to lysing enzymes was adapted from (Gerik et al., 2005). Briefly, overnight cultures of wild type and mutant strains in YPD medium were washed once with PBS and once with citrate buffer (10 mM, pH 6.0). Cells were resuspended in citrate buffer and the OD_{600}

was normalized to 1.0/ml with the same buffer. 1 ml aliquots were then subjected to centrifugation and the pellets (one per time point) were resuspended in a solution of lysing enzyme (final concentration 25 mg/ml; Sigma, L-1412) and incubated at 37°C with gentle agitation. At each desired timepoint one aliquot per strain was sedimented and resuspended in the same volume of distilled water (in the absence of lysis the OD_{600} should remain ~1.0). The assay was performed independently three times.

Mass spectrometry analysis

For total cellular proteome analysis, cells were collected by centrifugation at 3,500 rpm for 10 min and the pellets were washed twice with cold PBS before being subjected to acetone precipitation and enzymatic digestion (Geddes et al., 2016; Ball and Geddes-McAlister, 2019). For secretome analysis, supernatant fractions from *C. neoformans* WT and *sbh1*Δ cell cultures were collected and filtered using 0.22 µM syringe filters and subjected to in-solution trypsin digestion (Ball and Geddes-McAlister, 2019). Digestion was stopped by the addition of 10% v/v trifluoroacetic acid (TFA) and the acidified peptides were desalted and purified according to the standard protocol (Rappsilber et al., 2007). Approximately 50 µg of sample was loaded onto StageTips and stored at 4°C until LC-MS/MS measurement.

For LC-MS/MS measurement, samples were analyzed by nanoflow liquid chromatography on an EASY-nLC 1200 system (ThermoFisher Scientific) on-line coupled to a Q Exactive HF-X quadrupole orbitrap mass spectrometer (ThermoFisher Scientific). An in-line 75 µm x 50 cm PepMap RSLC EASY-Spray column filled with 2 µm C18 beads (ThermoFisher Scientific) separated peptides using linear gradients from 3% to 20% Buffer B (80% acetonitrile) over 18 min and from 20% to 35% Buffer B over 31 minutes, followed by a steep 2 min ramp to 100% Buffer B for 9 min in 0.1% Formic acid at a constant flow of 250 nl/min.

Raw files were analyzed together using MaxQuant software (version 1.6.0.26) (Cox & Mann, 2008). The derived peak list was searched with the built-in Andromeda search engine (Cox et al., 2011) against the reference *C. neoformans* H99 proteome downloaded from Uniprot (http://www.uniprot.org/) (Aug. 18, 2018; 7,430 sequences). The following parameters were included: trypsin enzyme specificity with a maximum of two missed cleavages, a minimum peptide length of seven amino acids, fixed modifications, including carbamidomethylation of cysteine, and variable modifications, including, methionine oxidation and N-acetylation of proteins and split by taxonomic ID. Peptide spectral matches were filtered using a target-decoy approach at a false-discovery (FDR) of 1% with a minimum of two peptides required for protein identification. Relative label-free quantification (LFQ) and match between runs were enabled; the MaxLFQ algorithm used a minimum ratio count of 1 (Cox et al., 2014). The mass spectrometry proteomics data have been deposited in the PRIDE partner repository for the ProteomeXchange Consortium with the data set identifier: PXD013894.

Statistical analysis of the MaxQuant-processed data was performed using the Perseus software environment (version 1.6.2.2) (Tyanova et al., 2016). Data were prepared by filtering for reverse database matches, contaminants, and proteins only identified by site, followed by $\log_2$ transformation of LFQ intensities. Filtering for valid values (three of four replicates in at least one group) was performed, and missing values were imputed from the normal distribution (width, 0.3; downshift, 1.8 standard deviations). A Student's *t*-test was performed to identify proteins with a significant differential expression (*p-value* < 0.05) (S_0 = 1) between samples employing a 5% permutation-based FDR filter.

In vitro macrophage survival assay

Fungal survival after engulfment by THP-1 (ATCC #TIB-202) cells *in vitro* was assessed as in (Santiago-Tirado et al., 2015) with only minor modifications: First, since the cryptococcal strains were grown in G418 for plasmid maintenance, they were washed extensively with PBS to remove all traces of drug before being opsonized, adjusted to an MOI of 10, and added to the THP-1 cells. Second, for CFU determination, 0.1% Triton-X100 (which had no effect on the cryptococcal cells) was used instead of SDS to lyse the THP-1 cells.

Infection studies

All animal studies were reviewed and approved by the Animal Studies Committee of Washington University School of Medicine and conducted according to the National Institutes of Health guidelines for housing and care of laboratory animals. Strains to be tested were cultured overnight in YPD medium, collected by centrifugation, washed in PBS, and diluted to 10^6 cells/ml in PBS for intranasal inoculation (50 µl) into 4-6 week-old female C57BL/6 mice (National Cancer Institute) that had been anesthetized with a combination of ketaset-HCl and xylazine. Initial inocula were plated to confirm CFUs. To assess long-term survival, infected animals were weighed 1 h post-infection and at least every other day afterwards. Mice were sacrificed if their weight fell below 80% of peak (an outcome which in this protocol precedes any signs of disease) or at the end of the study (10 weeks). To measure organ burden, infected mice were monitored as above for 14 days, at which point lungs and brains were harvested from all mice, homogenized in PBS, and serial dilutions of the homogenate plated on YPD agar for enumeration of CFU.

REFERENCES

Ball B, Geddes-McAlister J (2019). Quantitative Proteomic Profiling of *Cryptococcus neoformans*. *Curr Protocols Microbiology* 55:e94.

Cox J, Hein MY, Luber CA, Paron I, Nagarj N, Mann M (2014). Accurate proteome-wide label-free quantitation by delayed normalization and maximal peptide ratio extraction, termed MaxLFQ. Mol Cell Proteomics 13:2513-26.

Cox J, Mann M (2008). MaxQuant enables high peptide identification rates, individualized ppb-range mass accuracies and proteome-wide quantification. *Nature Biotechnol* 26:1367-72.

Cox J, Neuhauser N, Michalski A, Scheltema RA, Olsen JV, Mann M (2011). Andromeda: A peptide search engine integrated into the MaxQuant environment. J Proteome Res 10:1794-805.

Feng D, Zhao X, Soromani C, Toikkanen J, Römisch K, Vembar SS, et al (2007). The transmembrane domain is sufficient for Sbh1p function, its association with the Sec61 complex, and interaction with Rtn1p. *J Biol Chem* 282:30618-28.

Geddes JM, Caza M, Croll D, Stoynov N, Foster LJ, Kronstad JW (2016). Analysis of the protein kinase A-regulated proteome of *C. neoformans* identifies a role for the ubiquitin-proteasome pathway in capsule formation. MBio 7:e01862-15.

Gerik KJ, Donlin MJ, Soto CE, Banks AM, Banks IR, Maligie MA, Selitrennikoff CP, Lodge JK (2005). Cell wall integrity is dependent on the *PKC1* signal transduction pathway in *Cryptococcus neoformans*. *Mol Microbiol* 58:393–408.

Liu OW, Chun CD, Chow ED, Chen C, Madhani HD, Noble SM (2008). Systematic genetic analysis of virulence in the fungal pathogen *Cryptococcus neoformans*. Cell 135:174-188.

Rappsilber J, Mann M, Ishihama Y (2007). Protocol for micro-purification, enrichment, pre-fractionation and storage of peptides for proteomics using Stage Tips. Nat Protoc 2:1896-906.

Santiago-Tirado FH, Peng T, Yang M, Hang HC, Doering TL (2015). A single protein S-acyl transferase acts through diverse substrates to determine cryptococcal morphology, stress tolerance, and pathogenic outcome. *PLoS Pathog* 11(5):e1004908.

Skowyra ML, Doering TL (2012). RNA interference in *Cryptococcus neoformans*. *Methods Mol Biol* 845:165–86.

Toikkanen J, Gatti E, Takei K, Saloheimo M, Olkkonen VM, Söderlund H, de Camilli P, Keränen S (1996). Yeast protein translocation complex: Isolation of two genes SEB1 and SEB2 encoding proteins homologous to the Sec61ß subunit**.** *Yeast* 12:425-438.

Tyanova S, Temu T, Sinitcyn P, Carlson A, Hein MY, Geiger T, Mann M, Cox J (2016). The Perseus computational platform for comprehensive analysis of proteomics data. Nat Methods 13:731-40.

WT/mutant LFQ intensity (log2)	Protein IDs	Gene name	SP/TM	Protein function	Name
8.8143	J9VF18	CNAG_00776	SP1-22	mannoprotein MP88	MP88
8.4916	J9VVE4	CNAG_06000	TM466-89	glycoprotein, cellular response to dithiothreitol	
7.0869	J9VG30	CNAG_00164	SP1-25	alginate lyase-domain containing	
6.9625	J9VPN6	CNAG_05312	SP1-19	? (indicates note in orthology column at right)	
6.6036	J9VT92	CNAG_01231	SP1-20	agmatinase	
6.2588	J9VPI7	CNAG_05252	SP1-20	chaperone regulator	
6.2478	J9VL08	CNAG_00985	TM97-116	long chronological lifespan protein2	
6.2119	T2BNM4	CNAG_01314	SP1-20	vacuolar protein	
6.1804	J9VJA3	CNAG_05264	SP1-19	alpha-amylase	AMYA
5.8967	J9VSA9	CNAG_04869	SP1-17	carboxylic ester hydrolase	Pnb1
5.6773	J9VW39	CNAG_06459	SP1-18	vacuolar membrane protein	
5.6758	J9VXY3	CNAG_04753	?TM50-69	Gluconolactonase	
5.3417	J9VPL1	CNAG_03055	no	bud site selection protein 20	
5.2365	J9VDC2	CNAG_00150	SP1-23	serine endoptidase, cell wall	
5.1449	J9VND2	CNAG_01230	SP1-19	chitin deacetylase	Cda2
4.9877	J9VPM2	CNAG_05293		glycogenin glucosyltransferase	
4.8937	J9VPM4	CNAG_05893	SP1-16		
4.7309	J9VRE4	CNAG_04291	SP1-17	glycosyl hydrolase	
4.6703	J9VTM7	CNAG_06659	SP1-25	beta-hexosaminidase	Hex1
4.6317	J9VKV6	CNAG_01040	SP1-21	carboxypeptidase	
4.4586	J9VQU8	CNAG_04111	SP1-23	mannose-binding lectin	
4.3625	J9VWV9	CNAG_05502	TM136-60	DUF1996 domain-containing protein	
4.2684	J9VYJ6	CNAG_01519	no	endonuclease/exonuclease/phosphatase	
4.2591	J9VXD3	CNAG_01865	no	?	
4.2549	J9VMD9	CNAG_07629	SP1-21	vacuolar endopolyphosphatase	
4.2532	J9VXN6	CNAG_05595	SP1-18	Galactose oxidase, central domain	
4.2345	J9VFT3	CNAG_00074	TM95-120	protein PNS1	
4.1512	J9VTX0	CNAG_05731	SP1-23	glyoxal oxidase	
4.1332	T2BPG1	CNAG_04380	SP1-18	peptidase	
4.0744	J9VH90	CNAG_04033	SP1-23	alpha-1,3-glucosidase	
4.0743	J9VWV6	CNAG_04373	SP1-20	alginate lyase	
4.0351	J9VHN6	CNAG_02775	SP1-19		
4.0037	J9VUB8	CNAG_01653	SP1-19	cytokine-inducing glycoprotein	Cig1
4.0020	J9VR64	CNAG_04944	SP1-19	?	
3.9778	J9VIM6	CNAG_00290	SP1-22	amino peptidase	
3.9757	J9VTF2	CNAG_07856	SP1-19	Arylsulfotransferase	Bwc3
3.9754	J9VP43	CNAG_03940	no	elongator complex protein 2	
3.9452	J9VSR4	CNAG_01379	no		
3.9350	J9VPG8	CNAG_04085	no	oxidoreductase	
3.9177	J9VMR8	CNAG_00839	no	mitochondrial protein	

3.8630	J9W153	CNAG_01601	no	lipase	
3.8398	J9VS87	CNAG_02376	no	Identified spore protein 2	Isp2
3.8362	J9W1L8	CNAG_01778	SP1-24	?	
3.8205	J9VSY2	CNAG_03281	TM182-204	glycine-rich RNA binding protein	
3.8149	J9VPJ0	CNAG_03078	?TM79-101	type I phosphodiesterase/nucleotide pyrophosphatase	
3.7808	J9VDQ8	CNAG_00264	SP1-19	endonuclease	
3.7610	J9VVL8	CNAG_04785	no	stress-response A/B barrel domain protein	
3.7446	J9VH79	CNAG_00601	SP1-15	glycosyl hydrolase	Cel1
3.7070	J9VNQ8	CNAG_03829	no	L-carnitine dehydratase/bile acid-inducible protein F	
3.6826	J9VHV6	CNAG_00830	no	nuclear protein	
3.6756	J9VL58	CNAG_01172	SP1-18	beta-helix containing protein	Pbx1
3.6750	J9VMS8	CNAG_00854	TM29-46	sterol isomerase	Erg2
3.6410	J9VQ85	CNAG_03413	SP1-23	alginate lyase	
3.5829	J9VQD1	CNAG_03223	SP1-19	?	
3.5379	T2BPK2	CNAG_04782	TM32-51	phosphoesterase	
3.5342	J9VRC7	CNAG_06967	TM56-78	phytase	
3.5229	J9VQD3	CNAG_02189	SP1-21	alpha-amylase	
3.5128	J9W2F6	CNAG_06081	SP1-20	glucose oxidase	
3.5115	J9VHL5	CNAG_02811	no	small subunit ribosomal protein S29	
3.5046	J9VH59	CNAG_00581	SP1-19	saccharopepsin, vacuole	
3.4800	J9VZG6	CNAG_01854	TM77-99	heparinase familyII/III protein	
3.4553	J9VKN2	CNAG_02708	SP1-29	prenyl-cys oxidase/farnesyl lyase	
3.4399	J9VXZ9	CNAG_04735	SP1-19	extracellular metalloproteinase	Mep1
3.4072	J9VSG1	CNAG_02283	TM49-68	glucoamylase	
3.3827	J9VPB4	CNAG_00862	no	Rhodanese domain protein	
3.3725	J9VID8	CNAG_02754	no	40S ribosomal protein S12	
3.3661	J9VRT9	CNAG_02494	TM551-73	carboxypeptidase D	
3.3486	J9VWM8	CNAG_04269	SP1-16	peptide hydrolase	
3.3272	J9VK64	CNAG_02860	SP1-22	endo-1,3-beta-glucanase	Ebg1
3.3229	J9VTZ8	CNAG_00919	SP1-21	carboxypeptidase	
3.3117	J9VHM9	CNAG_02989	no	PX domain-containing protein	
3.2661	J9VH24	CNAG_02980	SA29-51	dipeptidase	
3.2309	J9VRU3	CNAG_07771	SP1-17	peptidase	
3.2288	J9VMZ0	CNAG_06745	no	histone H3	H3
3.1790	J9VV13	CNAG_02282	SP1-19	carboxypeptidase	
3.1102	J9VEG3	CNAG_00250	SP1-19	glyco-hydro-cc-domain-containing	
3.0441	J9VLU5	CNAG_00897	TM134-58	glucosidase	Skn1
2.9957	J9VJM5	CNAG_03063	no		
2.9897	J9W1W6	CNAG_05567	SA7-25	Ser/Thr-phosphatase	
2.9866	J9VNI6	CNAG_01169	SP1-18	aspartyl aminopeptidase	
2.9524	J9W0V0	CNAG_06351	TM72-92	protein transporter SEC61 subunit beta	

2.9507	J9VRJ3	CNAG_04346	no	dihydrodipicolinate synthase	
2.9155	J9VFF9	CNAG_00699	SP1-21	transmembrane receptor	Lpi15
2.8897	P82476	CNAG_01239	SP1-18	chitin deacetylase	Cda3
2.8672	J9W0T8	CNAG_06336	TM130-52	glucan-1,3-beta-glucosidase	
2.8603	J9VTM0	CNAG_01081	?SP1-19		
2.8252	J9VLJ9	CNAG_01019	no	superoxidase dismutase (Cu-Zn)	Sod1
2.7889	J9VVQ4	CNAG_02030	SP1-21	glyoxal oxidase	
2.7768	J9VMX6	CNAG_06760	no		
2.7690	J9W4A3	CNAG_05644	no	2-Nitropropane dioxygenase	
2.7662	J9VV30	CNAG_06107	no	G protein beta subunit-like	
2.7145	J9W0L4	CNAG_04625	SP1-17	cerevisin/proteinase B	
2.6784	J9VR40	CNAG_07442	SP1-20	phosphatidylglycerol/-inositol transfer prot.	
2.6511	J9VM07	CNAG_00600	SP1-33	capsular-associated protein	Cap60
2.6280	J9W1Z7	CNAG_05610	no	ER to Golgi transport	
2.6245	J9VQB6	CNAG_01331	SP1-18	?	
2.6241	J9VS16	CNAG_07782	SP1-24	oxidoreductase	
2.6115	Q6URB0	CCP1	no	cytochrome C peroxidase	
2.5874	J9W104	CNAG_06416	TM71-93	dipeptidyl aminopeptidase	Dap2
2.5518	J9VEK1	CNAG_00309	TM47-69	membrane protein	
2.5193	J9VQW9	CNAG_02592	no	thioredoxin reductase GliT	
2.5033	J9VV60	CNAG_02225	SP1-15	glucan-1,3-beta-glucosidase	Exg104
2.4889	J9VX79	CNAG_01794	no	2-hydroxyacid dehydrogenase	
2.4732	J9VLH9	CNAG_00407	SP1-16	glyoxal oxidase	
2.4372	J9VHI2	CNAG_00711	no	NTP transf 9 domain protein	
2.4025	J9VPN7	CNAG_03185	no	low temperature-responsive protein	
2.3984	J9VIH3	CNAG_02702	TM100-121	chloride channel	
2.3928	J9VQN4	CNAG_03353	?SP1-24		
2.3459	J9VPI7	CNAG_05252	SP1-20	chaperone regulator (also DMEM)	
2.3016	J9VJR6	CNAG_05193	TM345-67	ERGIC protein2	
2.2927	J9VPG5	CNAG_03146	SP1-25	alpha-amylase	
2.2897	J9VTG3	CNAG_03486	SP1-37	peptidyl-prolyl-isomerase	
2.2444	J9VRG7	CNAG_06694	no	5-hydroxy-isourate hydrolase	Uro2
2.1823	J9VTR9	CNAG_01637	TM30-50	COPII coat, Erv4	
2.1594	J9VL10	CNAG_01233	SP1-24	SH3-domain containing protein	
2.1586	J9VF55	CNAG_00588	SP1-16	ricinB-type lectin domain protein	
2.1216	J9VTM7	CNAG_06659	SP1-25	beta-hexosaminidase (also DMEM)	
2.0402	J9VTW8	CNAG_04130	no	Zn2 C6 domain protein	
2.0393	J9VWV6	CNAG_04373	SP1-20	alginate lyase (also DMEM)	
1.7358	J9VTW6	CNAG_05726	SA18-37	EMC3, ER	
1.7160	J9VSY5	CNAG_01307	SA 7-30	ER, Bap31	
-1.7660	J9VTS5	CNAG_01022	no	MATH domain protein	

-2.0254	J9VMA4	CNAG_00691	SA30-47	?	
-2.0657	J9VWI4	CNAG_04217	no	phosphoenolpyruvate carboxykinase (ATP)	
-2.1161	J9VKY8	CNAG_01000	no	nuclear pore complex protein Nup155	
-2.2177	J9VN55	CNAG_02131	no	iron-sulfur cluster assembly protein	Isa1
-2.2858	J9VGI4	CNAG_03753	no	dolichol-phosphate mannosyltransferase	
-2.3175	J9VQ01	CNAG_03321	no	vacuolar protein sorting-associated protein 9	
-2.4100	J9VZ46	CNAG_07598	no	importin-alpha export receptor	Cse1
-2.5312	J9VWV1	CNAG_04368	no	CD2 antigen cytoplasmic tail-binding protein 2	
-2.5770	J9VDV4	CNAG_00081	no	Pre-mRNA-processing factor 6	
-2.6249	J9VIX5	CNAG_03871	no	phosphotyrosine protein phosphatase	
-2.8171	J9VL09	CNAG_02567	no		
-2.9067	J9VKS6	CNAG_00148	no	Sec16	
-3.0856	J9VIF5	CNAG_07799	TM504-23	ABC transporter	
-3.1202	J9VTH7	CNAG_01126	no	guanine nucleotide exchange protein for ADP- robosylation factor	Sec7
-3.1426	J9VXG9	CNAG_05512	?TM588-608		
-3.2426	J9VN30	CNAG_02701	no	BAG domain protein	
-4.4577	J9W005	CNAG_05616	TM52-79	ABC transporter	
-4.5663	J9W155	CNAG_07943	TM138-60	ER protein, regulation of Ca++ entry	

Signal peptides and transmembrane domains of proteins induced in DMEM in KN99 (wild-type) *C. neoformans*

Transmembrane Domains (TM)

```
CNAG_06336          AQQKARSRKR  WFILLGGIILAVAAVVGIVVGVVV  SQVNKNDDDN
CNAG_01854          GFQPKKKRNK  WLWIGLPVLLICIILAAVLGGVL  GSRASNDNKD
CNAG_04782          PPRWRYLRSF  LPVIVLILLFFFLSSYSLLSH  SKSPAAKQH
CNAG_00309          SHNNVRSGTS  FAVRVTIATLIFLWTLLNINLVI SPFRQNSSISDL
CNAG_00074          RMNPRKRVNG  IIPLILFIAAVIGFAVVSGIAIHSFV QVNGLGGGMG
CNAG_00985          IKRNRIQTTG  VTMNLVLLAIFFFPLAFAQFGHF  FQQFGPFGG
CNAG_00897          DITSARGWAN  ALTLGILAGGGVMLFAGYPIISFYY  GDSNSSGANTSG
CNAG_00854          SASSTRCLKK  WSVRSLLVALLVSFYIWA  NTINHKFYILDPPS
CNAG_06967          RERSATRLTS  VLSRICIAFLIIVPTLAFAACYF  GRTTLDKVRTW
CNAG_02494          KGGNTDWEAW  YNAIFAFLVLGILVSIAGLYFYF  RRKPVSYRSRISLK
CNAG_02283          HRYRRVVIKG  LLLCLLILSAIVIRVSLGLW  PHYLNSRSVRFEH
CNAG_05502       KKRGCYPSTRRGR  LWFWGLIALTILAIVVIVAVCASVI  PKNNSSSDAT
CNAG_06416          RTRPRSKSRK  ILAILVAIIAFAGTIGVLAASGY  SAVPSFSSKGG
CNAG_06000          RHSILPPQPT  MLPLSLLPGLLALAPL ARAQVTATFPNAGAT
CNAG_06760          YRFSYTPTSP  LLFLYSALTHNPHKIHY  DQDWSVSKEE
CNAG_03078         RRGRGWITISG  FSLPKPLLYLLAIPPLLILINLIAS  TYNSARPHSHY
CNAG_03353          DRETILRPLR  LTGLLGGYNIFAFAC  GGGVSGQAGAVAL
CNAG_02592        SLVTKAIMSTTK  IDLLIIGGGPAGL  SAAITFSRLRRSC
CNAG_04753          GAKVLSWKSK  LVYAGFTMGALATLAYTASHIL  PSSSIAQASHL
CCP1                PSAPRSSNTG  YIFAGLGVAAVGAAYYFY  GTGRTEHDSTNKA
CNAG_02989         ARAEGQVGDLP  FLRFMFHQFLLPFPFLTA  APPTFWSAKVQPF
CNAG_00830       KFKGNNSSSSVEG  LLFMAFAAVQFLFWRVFM  RLDYQCPPHLTFT
CNAG_03063          SLSTNAGLPS  LQIIIPASSTVTLFIAFQ  PSVSLPPFPLSPL
CNAG_04085         RTVDWKTAKIG  IIGLGSIGSHLAFLLSSIGAT  SILYHSRRPSLHAA
CNAG_02702         RLIRRTLEEGE  AYVVISLVGVIIGVSAALISII  TTWLSDIKLG
CNAG_05193         VIRERTTSLYQ  FLIRLAGVVGGVWTVAAFALRV  FNRAQREVSK
CNAG_01637         TMEDVKIKTRT  GALLTFISLSIILTSVMLEFI  DYRRIHLEPS
```

Signal peptides and transmembrane domains of proteins induced in DMEM in KN99 (wild-type) *C. neoformans*

Signal Anchors (SA)

```
CNAG_05293          MSLPNA  FVTLLTTSSYLPGALVLLHALH  DLHPAPRDFQ
CNAG_02980      HLPSNRRRTS  ILLSLLALLLLLAAGLSLALVV  KHRHNEPTDFLE
CNAG_05567          MTARQT  IIIVSVVSLLLLYLFVHHI  TSSLEPSLPNAP
CNAG_05726      DLYLDPSIRD  WVLIPITLIMLLVGVLRHYV  TQFLNSAPKKQ
CNAG_01307          MTLYYS  ICFALLMSELSLFCTIVCPMPFAI  RKKMFHFLSE
```

Signal Peptides (SP)

```
CNAG_04735                MRSSALIALLPFLATLTAA  RPHHREDKHS
CNAG_02225                   MRLLIPFFIVPLAIA  RALPAFPTVD
CNAG_04869                  MRWLNIFPLLLPFVADA  SPLQPRRQAT
CNAG_05264                MPVLSNLISFLPFLAIAHA  ATSDEWRSRS
CNAG_00699              MLVNNLFYLIAALVTSAFVVA  QDDGWHIDYV
CNAG_02189              MLVHQAALALIPLFALLPVYA  LDADAMRSRS
CNAG_02030              MTSLNMATLLALLPLLSLVVA  SPSPTPQDGT
CNAG_03146           MLCCFCHRSLSVFNCLFVLRSPTRA  SLGKIEIPLL
CNAG_00581                MKTSAILIAALSAAASVEA  GIHRMKLEKQ
CNAG_07771                  MRARLLALLGLSGSVWA  TPALFTVEDM
CNAG_00407                   MYSAILLSLLPLLAAA  HRGPSRNLPN
CNAG_04269                   MLITPAILALPLLASA  VPTAREQLAF
CNAG_00290              MPSLLLPLILHLLSSLTNTAAA  AAVPPSSPAL
CNAG_00919                MCSKVVSAVLLAFALGSVI  EAAREPHGLR
CNAG_00264                MKLLPLALVVASTLPSALS  WGAAGHEMVA
CNAG_02775                MFALKSILVTSLITSTALA  HFTLDYPQRS
CNAG_03486 MNISHPIPTTMASRSFLSLLVALFVAICFVLSPGADA  AKGPVITNKV
CNAG_00264                MKLLPLALVVASTLPSALS  WGAAGHEMVA
CNAG_02189              MLVHQAALALIPLFALLPVYA  LDADAMRSRS
CNAG_07442               MKLVPLLIPFIATTVTASLA  GEALSWASQL
CNAG_04625                  MRFTAASLLLLPLAALA  SPIAQPSLAP
CNAG_00150             MVAFHASSALLSFALLATGFANA  FLSDDIKRGSDS
CNAG_00250                MLAANLISLVLVLPTLALA  RHNSPFNGHSPS
```

Signal peptides and transmembrane domains of proteins induced in DMEM in KN99 (wild-type) *C. neoformans*

CNAG_00776	MISKVAVGAAAALMAGVANVNA	QVTATGTMGPTN
CNAG_00588	MLFFATLLPLLALVSA	APFTKRYTGAKI
CNAG_00164	MTMLLGAFISSMICLLSHIPTAFA	FGLQNYPNLFF
CNAG_00601	MLFPALALLCPVLVA	AHGQLSWVQVGTGP
CNAG_04033	MIRSSLLWLTIIATLALLSLTLA	VKSEDFKQCSQ
CNAG_02860	MLVSNVVFPLFTLSFAVPAVSA	MRLNPAHAKR
CNAG_02708	MPPPSLTSSSTRFRVGFFVLLLAVSLSLT	HFTPSFTSHRS
CNAG_01314	MRFPLLLPFAALELPIPTAP	LEWKQANFLS
CNAG_01040	MWSKILTTALLVFALGSVVGA	ARDPLGLRGRR
CNAG_01233	MLPTFPRPISISSLLISFIHVSSI	TVVASTAAPA
CNAG_01172	MLFPLSLLLHLTSTVAA	ATTKCLVSGDQD
CNAG_00600	MPPQSFPLTVAPQTQRLAIRAALAILGLFILRA	LFSSSKSPEEIQSH
CNAG_07629	MRSRLLASLFTLALSVASSEA	ISSTGQMPLNG
CNAG_05567	MTARQTIIIVSVVSLLLLYLFVHHITSS	LEPSLPNAPSRD
CNAG_01230	MIPSTAAALLTLTAGAAFA	HTGCGGHEIGR
CNAG_01169	MAKASVVLFLSATTRSLA	RYLMKASIPFPP
CNAG_05252	MLPTTLFFLLTLALLGGCLA	ESLYSVLGVRK
CNAG_05893	MKYALFALALAGAVSA	QSNSTANSTESILI
CNAG_05312	MSSLHHLVPLLFLIAPALS	QYTATYSPSSLP
CNAG_03413	MSPFLTAALLSTLLSFVPSPVSA	VTLESIIDAYGLS
CNAG_01331	MLFGTLAYLALTITYGYS	LTVPQAHRETLE
CNAG_03223	MHSTAIIASFLASLALSNA	IKVESPNKDTV
CNAG_04111	MRRNPTLSLLSLTALTAISGVNA	AEPEDSLTSVI
CNAG_04944	MRSPGPSLLLLAALPLASA	THLSNKLQDKV
CNAG_04291	MLLPVITPLLLAAASYA	QQSTPRVLVYSAT
CNAG_07782	MTKSLYAFFSIILLFSVSSSVAA	SPQAQHHQHAMASS
CNAG_01231	MYGSLGVSILLMAATPIVLA	KIQEGGGYSQ
CNAG_07856	MLLPLIISTAIGVAPFARA	YLVNSSDYSSG
CNAG_06659	MLFNGLLEAVSLSLPFFASPSPLSA	KPDINVVPLPRH
CNAG_05731	MLSPLTLLHALSLAALAALPAQA	QLANTFQYVGLSGVSA
CNAG_01653	MIFNRFTFTAAMAASAASA	ISVQRRAQITD
CNAG_04380	MVNAHILTVLSILPLSLA	TLPEPDPHNGLSL

Signal peptides and transmembrane domains of proteins induced in DMEM in KN99 (wild-type) *C. neoformans*

```
CNAG_02282                MRTSPHTCVLLLCAASAIA  TPQHQAPIQLP
CNAG_06459                 MRSLSVFAIAICARSAVA  GQSPFTFGRAPQ
CNAG_04373               MLTSIIAALPLLASLPLSSA  YAVSDDAALES
CNAG_05595                 MFAVAALASLLSAIAVKA  VPCVQFDSSWNL
CNAG_01778           MFDFIITFFIAAAILAAVMALSVA  ITLPFAGALVRW
CNAG_06081               MLAPLALLPLLSLALPQVSA  DTRPGGLPHN
CNAG_01239                 MYGHLSLSALSLFAVVAA  APFRESWLQPRD
CNAG_02592     MPSLVTKAIMSTTKIDLLIIGGGPAGLSAA  ITFSRLRRSC
CNAG_01081                MKVIVLGASGFIGHRVALA  FVQAGHFVWG
CNAG_01601         MYIPGPLRLSSYFLPFISSPSPPAQS  SPDTRTISFKP
```